Characterization of the *Smpec* Knock-out mouse

Latifa Aljebali, MSc.

Department of Human Genetics
McGill University
Montreal, Quebec, Canada

April 2013

A thesis submitted to McGill University in partial fulfilment of the requirements of the degree of Masters of Science

Table of contents

Abstract

The *Smpec* gene is expressed solely in the chondrocytes at the resting and proliferating zones but not in the hypertrophic chondrocytes. The SMPEC protein is a chondroitin sulfate proteoglycan (CS PG) composed of 121 amino acids. In silico analysis suggests it is a transmembrane protein. The purpose of this study was to characterize the *Smpec* knockout (KO) mouse and identify its role in skeletogenesis in vivo. To confirm the suggested topology for the SMPEC protein, immunofluorescence (IF) was performed on 4 days post natal (P4) distal femur. The protein was localized to the cell surface of resting and proliferating chondrocytes, but also accumulated in intercolumnar septum of hypertrophic chondrocytes, suggesting its shed. Alcian blue /alizarin red staining, which stains cartilage and bone respectively, was performed on arms of P4 wild-type (WT) and KO mice and there were no qualitative differences in staining intensity neither in bone nor in cartilage of KO compared to WT. However, quantitative measurement indicated that the humeri were all statistically reduced in length by 10.4% in the KO compared to the WT. As it is well known that the longitudinal growth of long bones is mediated through the growth plate, thereby we focused our study on this region. Safranin O/Fast green staining in P4 distal femur revealed that the chondrocyte cell density of the resting and proliferating zones appeared less in the KO than in WT littermates. Quantitative analysis confirmed the hypocellularity of these zones. However, the thickness of the hypertrophic zone was normal. The expression profile of genes known to be important in skeletogenesis and mineralization was assessed by real-time qPCR. No statistically significant changes were detected in the *Smpec* KO as compared to WT at the three ages analyzed (day 4, day 28 and 12 months). Similarly, primary chondrocytes cultures established from KO and WT rib cages, did not present any significant changes in expression of *Col2a1*, *Col10a1*, *Sox9*, and *Acan*. Furthermore, in such cultures, extracellular matrix deposition of proteoglycan aggrecan as assessed by alcian blue staining, was not significantly altered, indicating

similarity in the metabolic activity of the chondrocytes. This indicates for the first time that loss of *Smpec* results in mild dwarfism in mice and that its function cannot be compensated by other genes at least at neonatal ages. The mechanism by which the lack of SMPEC causes dwarfism is still unclear.

Résumé

Le gène *Smpec* est exprimé uniquement dans les chondrocytes de la plaque de croissance à l'exception de la zone hypertrophiée. La protéine SMPEC est une protéoglycane contenant de la chondroïtine sulfate (CS PG) et composée de 121 acides aminés. Une analyse in silico indique qu'il s'agit d'une protéine transmembranaire. Le but de cette étude était de caractériser le phénotype d'un modèle de souris dont le gène *Smpec* a été inactivé (KO), en particulier l'effet sur la formation du squelette. Pour confirmer la topologie proposée pour SMPEC, elle a été localisée par immunofluorescence (IF) sur des fémurs au jour 4 postnatal (P4). La protéine est présente à la surface de la cellule dans la zone superficielle et la zone de prolifération. Par contre, elle s'accumule aussi dans la matrice extracellulaire de la zone hypertrophiée, entre les colonnes de chondrocytes. Ce résultat suggère que le domaine extracellulaire est coupé et libéré dans la matrice à la zone de transition. Une coloration avec le bleu alcian et l'alizarine rouge, a été réalisée pour visualiser le cartilage et l'os dans les humérus au jour 4 postnatal. Aucune différence qualitative dans l'intensité de la coloration, ni dans les os ni dans le cartilage n'a été détectée dans la souris KO par rapport à la souris sauvage. Cependant, une mesure quantitative a révélé que plusieurs parametres osseux sont significativement diminues dans le KO, entre autre la longueur totale qui est reduite de 10.4% par rapport a la souri sauvage. Étant donné que la plaque de croissance est responsable de la croissance longitudinale des os longs, nous avons ensuite plus spécifiquement investigué cette région. Une coloration avec la safranine O a permis de révéler la densité cellulaire dans les zones superficielle et de prolifération était diminuée dans la souris mutante. Cependant, l'épaisseur de la zone de

chondrocytes hypertrophiés est demeurée inchangée. Le profil d'expression de plusieurs gènes connus pour être importants dans squelettogenèse et la minéralisation est aussi restée inchangée dans les plaques de croissance isolées à partir des femurs in vivo, et dans les cultures de chondrocytes in vitro. Aussi, les depots de proteoglycan aggrecan dans la matrice extracellulaire in vitro n'a pas été modifiée indiquant la similitude de l'activité métabolique des chondrocytes KO et sauvages. Ceci indique pour la première fois que la perte de fonction du gène *Smpec* in vivo cause un nanisme léger, mais que le mécanisme en cause demeure indéterminé.

Acknowledgments

I would first like to thank my supervisor, Pierre Moffatt, for his guidance, advices and open-door policy. He has helped me tremendously with the progression of this research. I am proud to be under his supervision.

I would also like to thank my supervisory committee members, Dr. St-Arnaud and Dr. Roughley, for their valuable comments and suggestions to keep me on track. I am very grateful to them. Many thanks to Marie-Helene for helping me master lab techniques and for her company in the lab.

Also, I would like to thank the Ministry of Higher Education and King Saud University, for scholarship and funding during my master study.

Lastly, I would like to express gratitude to my mother for her endless support and encouragement. It is to her that I owe all my accomplishments.

List of Abbreviations

ACAN: Aggrecan

ANK: Progressive ankylosis

BrdU: 5-bromo-2'-deoxyuridine

chABC: Chondroitinase ABC

chB: Chondroitinase B

chACI: Chondroitinase ACI

chACII: Chondroitinase ACII

COL2A1: Collagen type IIα1

COL10A1: Collagen type Xα1

CS: Chondroitin sulfate

DS: Dermatan sulfate

E: Embryonic day

ECM: Extracellular matrix

ENPP1: Ectonucleotide pyrophosphatase/phosphodiesterase 1

HS: Heparan sulfate

IF: Immunofluorescence

IHC: Immunohistochemistry

IHH: Indian hedgehog

ITS: Insulin-transferrin-selenium

GAG: Glycosaminoglycan

KO: Knockout

KS: Keratan sulfate

Lac-Z gene: Bacterial β-galactosidase

MGP: Matrix gla protein

MMP: Matrix metalloproteinase

OA: Osteoarthritis

OPN: Osteopontin

P: Post-natal day

PBS: Phosphate buffered saline

PFA: Paraformaldehyde

PCR: Polymerase chain reaction

PG: Proteoglycan

PPi: Inorganic pyrophosphate

PRG4: Proteoglycan 4

Runx2: Runt-related transcription factor 2

SMPEC: Small membrane protein expressed in chondrocytes

SOX9: Sex determining region Y box 9

SYND: Syndecan

TIMP: Tissue inhibitor of metalloproteinases

TNAP: Tissue non-specific alkaline phosphatase

VEGF: Vascular endothelial growth factor

WT: Wild-Type

List of Figures and tables

I. Introduction

I.1 Skeletogenesis

The skeletal system is one of the most important systems for vertebrae, which provides a framework for the body to support and protects internal organs and is essential for movement. It is the location for blood cell formation and an important storage reservoir of calcium and phosphate (1). The skeletal system is composed of cartilages and bones and has at least five cell types: chondrocytes in the cartilage and osteoblasts, osteocytes, osteoclasts and bone lining cells in the bones (2). During embryogenesis, bones develop in two ways. The first is called endochondral ossification in which a cartilage template is first formed by chondrocytes then gradually ossified by osteoblasts. This process occurs in most skeletal elements and the resulting bone is called an endochondral bone. The second is called intramembranous ossification where mesenchymal stem cells differentiate directly into osteoblasts which lay down the mineralized bone. This type of bone is called membrane bone (1-3).

I.2 Cartilage

Cartilage is the first skeletal tissue formed during embryonic development (4). It is a non-mineralized connective tissue which does not have blood vessels, neural or lymphatic vessels (5). It gains nutrients and discards waste by diffusion from and to blood vessels surrounding it. In an adult, it is present in the nose, ear, bronchial tube, rib cage, intervertebral discs and in joints between bones (1 and 5). Depending on the morphology and the extracellular matrix (ECM) composition, cartilage is classified into three types: hyaline, elastic and fibrous. Hyaline cartilage is the most abundant type forming most of the embryonic skeleton. The matrix of hyaline cartilage is composed of collagen type II (COL2A1) and chondroitin sulfate (CS). In adults, it is present in the nose, trachea and costal cartilage of the ribs. Elastic cartilage matrix has

elastic fibers (thus the name) as well as COL2A1. This type of cartilage is present in the ear and epiglottis. The fibrous cartilage is located in the intervertebral discs, knee joint and pubic symphysis. Although its matrix composition is similar to that of the hyaline cartilage, it also has collagen type I (1, 5 and 6).

I.3 Bone development and growth

In chondrogenesis, mesenchymal cells are differentiated to chondrocytes. These chondrocytes proliferate and differentiate, forming cartilage anlagen (5 and 7). In embryonic stage, this anlagen serve as a template for endochondral bone development which involves terminal differentiation of the chondrocytes, mineralization of the matrix and blood vessels invasion (8 and 9). Typically the ossification process takes place in the center (diaphysis) of the cartilage anlagen in a region called primary ossification center. In this region bone collar forms around the cartilage template, the diaphysis calcifies and a cavity is formed. These cavities are invaded with blood vessels, lymphs, nerve fibers, red marrow elements, osteoblasts and osteoclasts. These cavities are the sites for spongy bone formation (1). As the primary ossification center enlarges, the newly formed spongy bone is degraded by osteoclasts which in turn open up a medullary cavity in the center of the diaphysis. As this process continues, the developed bone has a bony diaphysis surrounding remnants of spongy bone and a widening medullary cavity restricting two cartilages at the ends (epiphyses) (1, 4, 8 and 10).

In early postnatal stages, secondary ossification centers appear in one or both epiphyses. This process has almost the exact same sequence of events of primary

ossification except that no medullary cavity forms in the epiphyses. Upon completion of the secondary ossification, the cartilage remains only at two sites: on the epiphyseal surfaces, as articular cartilages, and at the junction of the diaphysis and epiphysis (not in humans), forming the growth plates (1, 4, 8 and 10).

The articular cartilage is a hyaline cartilage found at the surface of all long bones facing the joint which remains during adult life. It consists of three pseudo stratified zones: the superficial, intermediate and deep layers. The articular chondrocytes synthesize a non mineralized matrix ideal for its function which is to reduce friction and absorb loads (5, 8 and 11).

The epiphyseal growth plate develops at each end of a long bone. Each growth plate consists of three distinct zones: resting, proliferating and hypertrophic (Figure 1). Each zone differs in the maturation stage of chondrocytes, ECM composition and morphological appearance (12-14). The growth plate is responsible for longitudinal growth until the bone is fully developed. This is accomplished by three mechanisms. First, through proliferation which produces more cells. Second, through matrix formation and third through the increase in cell size during hypertrophy (15).

The chondrocytes of the resting zone are spherical and randomly scattered (Figure 1A). This zone is located closest to the articular surfaces. It provides a reservoir of chondrocytes to the differentiation pathway (12-14). The proliferating zone is composed of flat chondrocytes arranged in longitudinal columns, parallel to the axis of growth and produce large amounts of ECM containing COL2A1 and aggrecan (ACAN) (Figure 1B). Those chondrocytes undergo active division, a

process responsible for the bone growth (12-14). The hypertrophic zone contains enlarged chondrocytes which are terminally differentiated and exit the cell cycle in the osteochondral junction (Figure 1C). Hypertrophy is the most important contributor of the longitudinal growth. They secrete the vascular endothelial growth factor (VEGF), which results in blood capillary invasion and express collagen type Xα1 (COL10A1). This is followed by chondrocyte apoptosis, to be replaced by osteoblasts (12-14, 16 and 17). One of the main features of chondrocytes is that they are metabolically active and synthesize a large amount of matrix components including collagens, glycoproteins and proteoglycans (PG) (15).

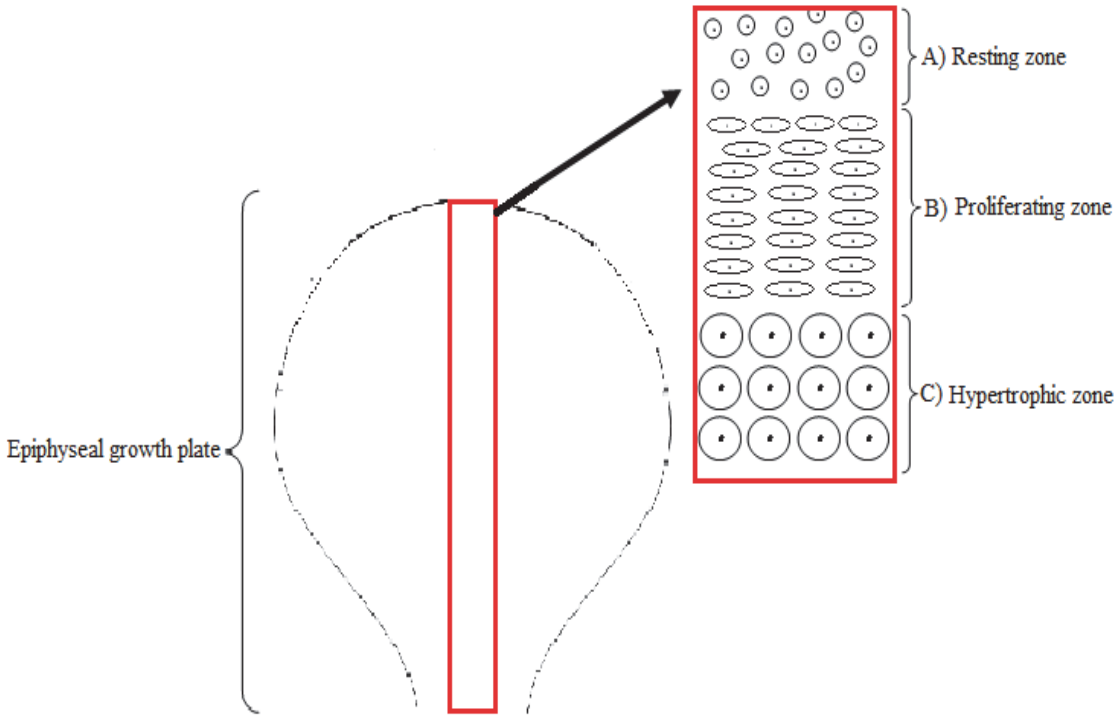

Figure 1: Schematic representation of the growth plate zones. (A) The resting zone chondrocytes are spherical and randomly distributed. (B) The proliferating zone chondrocytes are flat and arranged in a longitudinal columns. (C) The chondrocytes of the hypertrophic zone are enlarged and terminally differentiated. Adapted from 5 and 9.

I.4 Proteins important for cartilage and bone

Development of the skeleton is a multistep tightly regulated process which involves a vast number of transcription factors, growth factors and ECM proteins (7). In the following paragraphs I will describe a selected set of molecules expressed in the growth plate that are pertinent to the context of the current study. These molecules have different functions essential for growth plate establishment and are involved in the ECM formation and mineralization regulation.

I.4.1 Sex determining region Y box 9

Sex determining region Y box 9 (SOX9) is a transcription factor belonging to the Sox family, which has a high mobility group box DNA binding domain. SOX9 has a potent transcriptional activation domain, which binds selectively to the minor groove of DNA (11, 18-22). It is expressed from condensed mesenchymal cells, resting and proliferating chondrocytes (11 and 12). It is important for inducing the expression of *Col2a1* and *Acan* (4, 12, 18 and 23). Humans with *SOX9* heterozygous mutations suffer from Campomelic dysplasia disease. These patients are characterized by hypoplasia of the endochondral skeletal elements. In addition, homozygous mutations in *SOX9* result in complete cartilage synthesis inhibition (24-26). Generation of a mouse model with homozygous mutations in *Sox9* was not possible since the heterozygous *Sox9* mice die at birth. To circumvent this problem, *Sox9* homozygous mutant embryonic stem cells, in which the *lac-Z* gene replaces the *Sox9*, were injected into wild-type (WT) blastocysts. It was found that *Sox9* null cells do not contribute to the chondrogenic mesenchymal condensations and lack the ability of

expressing *Col2a1* and *Acan* (18). Therefore, SOX9 is defined as a master regulator of chondrogenesis.

I.4.2 COL2A1

COL2A1 is a secreted protein of the collagen family. It is a homotrimer of COL2A1 forming a triple helix molecule. It is expressed in different tissues including the eye vitreous, vertebral discs, ear tectorial membrane and cartilage (4, 27 and 28). It accounts for about 80% of the total collagen content in the cartilage, thus termed "collagen cartilage". It is classified as a fibril-forming collagen which is the major source of the fibrillar matrix in the articular cartilage (29). The fibril-forming collagen assembles into highly aligned supramolecular aggregates. Due to the high content of hydroxylysine, glucosyl and galactosyl residues in COL2A1 protein, it has the ability to interact with PG, which are present in the cartilage matrix (30). This fibrous network prevents the hydrophilic PG from being overswelled (31). In 1988, a heterozygous mutation for COL2A1 chain was found in patients with a Chondrogenesis type 2, which is characterized by a lethal perinatal form of short-limbed dwarfism (32). Moreover, it is associated with early onset Familial osteoarthritis (OA) (33-35). Other studies demonstrated that mutations in the *COL2A1* gene resulted in Kniest dysplasia (36-38). Accordingly, COL2A1 is very important for normal skeleton development.

I.4.3 COL10A1

COL10A1 is a secreted protein of the collagen family. It is a homotrimer triple helix with long C-terminal and a short N-terminal domain, coded by *Col10a1* gene (39). It is classified as hexagonal network-forming collagens (29). It is expressed specifically in hypertrophic chondrocytes thus used as a marker to label this zone. Zheng et al. concluded that runt-related transcription factor 2 (RUNX2) binds the promoter of *Col10a1* during chondrogenesis (40). It is well known that RUNX2,

expressed by prehypertrophic chondrocytes, is required for chondrocyte hypertrophy (41 and 42). In humans, a mutation in the *COL10A1* gene causes Schmid metaphyseal chondrodysplasia (43-45). In 2007, a study on mice harboring the equivalent of a human 1859delC frame shift mutation demonstrated typical phenotypes of Schmid metaphyseal chondrodysplasia, including short limbs (45). An in vivo study revealed that Spondylometaphyseal dysplasia in mice was seen in a transgenic dominant-negative mutation in *Col10a1* (46). However, null *Col10a1* mice had normal long bone development and growth (47). This suggests that the dominant negative mutation, rather than the absence of COL10A1, is harmful for the cells. The proposed common consequence of these mutations is the improper trimerization and secretion of the COL10A1 (48).

I.4.4 Alkaline phosphatase

The alkaline phosphatase family are hydrolytic enzymes which dephosphorylate substrate molecules. In humans, the family is composed of four isozymes: the placental, placental-like, intestinal and tissue non-specific (liver, kidneys and bones) (49). The tissue non-specific alkaline phosphatase (TNAP) is a glycosylated membrane bound enzyme which has a broad specificity that cleaves phosphate groups from phosphate ester compounds (50). The *Tnap* is expressed by osteoblasts of bone thus used as a marker for bone formation (51 and 52) and also expressed in hypertrophic chondrocytes (53). It is known that osteoblasts are involved in the mineralization of the matrix by forming the hydroxyapatite which is composed of calcium and phosphate (54). Studies on human and animal models revealed the importance of the TNAP. An infant male who died with Hypophosphatasia at 3 months of age had a homozygous mutation in the *TNAP* gene (55). More studies were

published on identifying different mutations in the *TNAP* gene in Hypophosphatasia patients (56-60). Mutations in *TNAP* have been reported in three patients with Odontohypophosphatasia (61). In summary, deactivating mutations in the *TNAP* gene cause Hypophosphatasia which is characterized by defective bone mineralization. It is manifested as rickets in cartilage and osteomalacia in bones and elevated extracellular inorganic pyrophosphate (PPi) (56). It is well known that extracellular PPi inhibits the formation and growth of the hydroxyapatite crystals and promotes calcium pyrophosphate dehydrate (CPPD) crystals (62 and 63). There are at least three factors regulating the level of the extracellular PPi: the rate of its synthesis, transport across the cell membrane and its degradation rate (64). The TNAP enzyme catalyses the PPi hydrolysis which in turn decreases the level of the extracellular Pi. This hydrolysis promotes hydroxyapatite crystals formation (62 and 63).

I.4.5 Progressive ankylosis

Progressive ankylosis (ANK) is a multiple pass transmembrane protein. It is expressed by hypertrophic chondrocytes, perichondrium cells, periosteum cells and tendons (65 and 66). It transports the intracellular PPi to the extracellular milieu. Extracellular PPi is a major inhibitor of physiological and pathological calcification, bone mineralization, and bone resorption (65). Non functional ANK results in intracellular PPi accumulation and reduction in the concentration of the extracellular PPi. This promotes pathological calcification (65). Mutations in the *ANK* gene are found in patients with Craniometaphyseal dysplasia characterized by widening of the bones (67-69) and Chondrocalcinosis a disorder manifested by calcification of

cartilage and/ or soft tissues (64, 70-74).

I.4.6 Ectonucleotide pyrophosphatase/phosphodiesterase 1

Ectonucleotide pyrophosphatase/phosphodiesterase 1 (ENPP1) is a cell membrane bound glycoprotein, a member of the ecto-nucleotide pyrophosphatase / phosphodiesterase (ENPP) family (75 and 76). It is a hydrolytic enzyme with broad specificity which converts nucleoside 5' triphosphates to their corresponding monophosphate and PPi (77). It is present in the plasma membrane of hepatocytes, renal tubules, salivary duct epithelium, epididymis, capillary endothelium in the brain, chondrocytes and osteoblasts. It has a vital role in regulating pyrophosphate levels and bone mineralization (75-78). Mutations in the *ENPP1* gene are found in patients with arterial calcification (79-84), ossification of posterior longitudinal ligament of the spine (85-87) and Chondrocalcinosis (64). This explained the role of ENPP1 enzyme as a physiological inhibitor of calcification. Blocking the ENPP1 hydrolysis activity affects the rate of PPi synthesis (64). This eliminates the inhibitory effect of the PPi on calcification.

I.4.7 Matrix gla protein

Matrix gla protein (MGP) is a secreted insoluble matrix protein of the vitamin k dependent family. It is expressed by the heart, kidneys and lungs and is induced by vitamin D in bones (88). The MGP is secreted from chondrocytes and vascular smooth muscle cells with abundant aggregation in bones, dentin and cartilage (89). It inhibits the calcification of cartilage and arteries (90) through binding calcium ions and hydroxyapatite with its γ-carboxylation glutamic acid residues (91). It requires

the γ-carboxylation of its five glutamic acid residues for its biological activity (92) as inhibition of this carboxylation resulted in increased matrix calcification (93 and 94). Mutations in the *MGP* gene found in patients with Keutel syndrome, characterized by cartilage calcification (95 and 96). Moreover, *Mgp* knockout (KO) mouse has disorganized growth plate in which proliferative chondrocytes fail to form columns and there were no hypertrophic chondrocytes (90).

I.4.8 Osteopontin

Osteopontin (OPN) is a secreted protein of the small integrin-binding ligand N-linked glycoprotein (SIBLING) family (97). It undergoes post-translational modification which involves phosphorylation (98 and 99), glycosylation (100 and 101), sulphation (102) and transglutaminase cross-linking (103). The protein has a high content of aspartic and glutamic acid as well as serine. It also has a poly aspartic acid motif which gives it the ability to bind to the hydroxyapatite and calcium ions as well as an Arginine-Glycine-Aspartate (RGD) sequence which can stimulates cell attachment (98-100 and 104-106). It is expressed in different tissues including bone, cartilage, dentin, brain, kidneys, gastrointestinal tract, gall bladder, pancreas and vascular tissue (107 and 108). In bone and cartilage, it is expressed by osteoblasts, osteoclasts and hypertrophic chondrocytes (109-111). It has been found that OPN represses hydroxyapatite formation, promotes angiogenesis, osteoclast aggregation and bone resorption (112). The repression effect of OPN is mediated by binding the hydroxyapatite crystals which revealed the importance of OPN in preventing soft tissue calcification (113).

I.5 PG

PG are glycosaminoglycans (GAG) linked to core proteins. Some of them are listed in Table I with characteristic features. They are classified according to the sugar moiety they contain: CS, keratan sulfate (KS), dermatan sulfate (DS) and heparan sulfate (HS) (114). The PG differ in the amino acid sequence of the core protein and by the type and number of GAG chains they have (115). The GAG is composed of a linear polymer of disaccharide unit repeats. They are categorized into glucosaminoglycan including KS and HS and galactosaminoglycan, involving CS and DS (116). These sugars are added post-translationally in the Golgi to serine residues onto core proteins moiety and can be further extensively modified in subsequent steps that lead to at least sulfation and epimerization. These extensive modifications result in massive molecular diversity and complexity (114). The PG are found in most tissues and organs of vertebrates (117) and the PG in cartilage are summarized in table I (114 and 117-120). Studies of PG reveal their vital physiological, homeostatic and developmental roles (114). They are either secreted (ACAN and perlecan), or presented on the cell membrane (syndecans and glypicans) (116). PG have different functions such as water retention and interaction with and control of the activity of many other secreted factors important for growth plate development. The interaction of these factors with selected PG can either limit their diffusibility, modulate their presentation to cell surface receptors, and/or protect them from degradation (118 and 121-126). Defects in biosynthesis of core protein, GAG chain, enzymes involved in

the synthesis or modification of GAG chains are associated with a variety of syndromes, some of which can be lethal (reviewed in 114).

Table I: Cartilage Proteoglycans. List of cartilage PG indicating their GAG chain type and localization. Adapted from 114, 117 and 118.

PG name	GAG chain	Tissue location
Fibromodulin	KS	Extracellular, intracellular
Lumican	KS	Extracellular
proline/arginine-rich end leucine-rich repeat protein (PRELP)	KS	Extracellular
Aggrecan	CS/DS	Extracellular
Versican	CS	Extracellular
Biglycan	DS/CS	Extracellular
Decorin	CS/DS	Extracellular
Epiphycan	DS/CS	Extracellular
CD44	CS/DS	Transmembrane, extracellular, Intracellular
Syndecans	HS	Transmembrane, extracellular
Glypicans	HS	Cell surface
Perlecan	HS	Extracellular

I.5.1 ACAN

ACAN is a PG secreted in the ECM (117). The GAG in the ACAN are composed of KS and CS and require more than 30 enzymes for its post-translational modifications (118). It is the most abundant PG in the ECM of the cartilage (5). It is expressed by the resting and proliferating chondrocytes under the influence of *Sox9* (18 and 127). Defects in the *ACAN* gene in humans are found in patients with Spondyloepiphyseal dysplasia type Kimberley (SEDK) which is characterized by short stature (128), Spondyloepimetaphyseal dysplasia aggrecan type which is characterized by severe short stature and facial dysmorphism (129), and Osteochondritis dissecans short stature and early-onset OA (130). Moreover, a study on animal model revealed that mutations in the *Acan* gene are the cause of cartilage matrix deficiency in mice (131 and 132) and Chondrodysplasia (133). This reveals the pivotal role of ACAN in normal skeleton development and maintenance. The protein ACAN is highly anionic and thus binds to cations and water, which in turn creates osmotic pressure and swelling, providing cartilage with its viscoelastic properties (134). The ACAN core protein binds non covalently to COL2A1 and hyaluronan forming aggregates which connect ECM with cell surfaces (118). Moreover, it has been found that ACAN binds to Indian hedgehog (IHH), a regulator of chondrocytes proliferation and osteoblast differentiation which is expressed by prehypertrophic chondrocytes and osteoblasts (12 and 135), via its CS chains (126). This suggested that ACAN establishes an IHH morphogen gradient in the epiphyseal

growth plate (136). This gradient is necessary to drive the process of cell differentiation proportionally with the morphogen concentration (126).

I.5.2 Proteoglycan 4

Proteoglycan 4 (PRG4) is a secreted glycoprotein containing CS and KS GAG (137 and 138). It is expressed by synovial tissue, superficial zone chondrocytes of the articular cartilage, liver, heart and lungs (139). It is the major component of synovial fluid involved in cartilage surface protection and prevention of synovial cells overgrowth (140). Its expression elevated as the joint matures, suggesting it has a functional rather than a developmental role (140). Human mutations in *PRG4* cause Camptodactyly- arthropathy- coax vara -pericarditis syndrome which is characterized by joint failure (141). Aged mice lacking PRG4 develop tendon sheaths calcification, loss of superficial chondrocytes and hyperplastic synoviocytes. This indicates that PRG4 provides cytoprotection of tendon as its absence resulted in tissue damage, remodeling of the matrix and dystrophic calcification. It also suggests that the lack of PRG4 function causes a loss of the superficial chondrocytes probably due to increased friction. Moreover, PRG4 controls the synoviocytes growth and inhibits the adhesion-dependent cell growth, as hyperplastic synoviocytes destroy cartilage surfaces. This indicated the vital role of PRG4 in long term joint homeostasis (140).

I.5.3 Syndecans

Syndecans (SYND) are a family of type I transmembrane HSPG (142). The core protein has a cytoplasmic domain at the C-terminal which is shared by all the family members, a single transmembrane domain and extracellular domain at the N-terminal

which is unique for each member of the family with site (s) susceptible for protease cleavage (143). In vertebrates the family has four members: syndecan1 (SYND1), syndecan2 (SYND2), syndecan3 (SYND3) and syndecan4 (SYND4) (144). Although all cells except erythrocytes express at least one member of the SYND family, each member has a tissue specific and developmentally regulated expression (144 and 145). In mice tissues, *Synd1* is expressed from the ectoderm during gastrulation then localized on mesodermal cells. It is permanently expressed by epithelial cells and upregulated in articular cartilage during cartilage degradation OA. *Synd2* is constantly expressed by perichondrial, periosteal and connective tissue cells (144). *Synd3* is abundant in the limb buds, brain, neural tube (144) and in chondrocytes of the proliferating zone during growth plate maturation (118). *Synd4* is expressed from cartilage tissue during embryogenesis in mice. It is highly expressed by proliferative, hypertrophic chondrocytes and epiphyseal cartilage during endochondral ossification. *Synd4* is also upregulated in human and mouse articular cartilage during OA (144).

SYND are involved in a variety of functions. They serve as adhesion molecules, binding chemokines, cytokines, growth factors, morphogens, pathogens and matrix metaloproteinases (MMP) (143 and 144). This binding is mediated through the core protein as well as the GAG chains (134). SYND bind with fibronectin through their heparin binding domain medicate cell adhesion (143). If this binding is interfered with tenascin C, the cells will not adhere and that will promote tumor cell proliferation (144). SYND4 possesses a protein kinase C (PKC) motif in its variable region which regulates the expression of cell adhesion molecules including

fibronectin and its integrin receptor. Thus SYND4-fibronectin interaction promotes focal adhesion formation and reorganization of the actin cytoskeleton. It is also associated with up regulating the expression of MMP, integrins and down regulating *Col2a1* expression, thereby it mediates cartilage matrix degradation as in the case of OA (144). This is consistent with the significant reduction in cartilage PG loss and thereby severity of OA in the *Synd4* deficient mice (144). On the other hand, SYND have the ability to bind pathogens like human immunodeficiency virus1 (HIV1), HIV2, herpes papilloma virus, simian immunodeficiency virus, and hepatitis C virus through their anionic HS chains (143). These pathogens use SYND as receptors which assist their entry into host cells or permanence in the hostile host environment (143).

In addition to these activities, SYND can bind to morphogens and restrict their availability to the receiving cells as well as their loss in the extracellular space, thereby creating a morphogen gradient. SYND3 binds to the morphogen IHH which promotes chondrocytes proliferation (144).

SYND undergo regulated proteolytic cleavage, at the variable domain, in a process known as shedding (145), which is mediated through external factors such as plasmin, thrombin and MMP (144). This cleavage generates a soluble HSPG that can competes with the intact SYND for the ligand binding via its GAG chains (144), and the remaining portion of the membrane bound receptor fails to bind ligand (145). Both SYND1 and SYND4 are shed by MMP after injury which promote cell migration and assist wound healing (144 and 145). Therefore, MMP have a pivotal

role in normal matrix turnover and reproduction as well as in pathological remodelling in inflammation, cancer invasion and metastasis. SYND are protected from MMP by binding with tissue inhibitor of metalloproteinases (TIMP) via their GAG chains (145).

I.5.4 SMPEC a novel PG

Although in the last few years much has been learned about the mechanisms that regulate the formation of skeletal tissues, novel genes are still being identified and studied. Among those is *Smpec* (Small membrane protein expressed in chondrocytes) which was identified by our group in 2002 from a screen of an embryonic mouse (E) 14.5 limb cDNA library encoding secreted and membrane protein through a gene trap technology (146). It was originally named *C2ORF82* in humans, whereas in mice, it corresponded to the *Riken clone 3110079O15* (GenBank NM_028473.1). From the initial data generated by our group, SMPEC is a CSPG, expressed specifically by chondrocytes. The gene encoding *Smpec* is located on mouse chromosome 1, spans 5.2kb and is composed of 3 exons (Figure 2A). Cloning of the mouse *Smpec* full length cDNA revealed it is a small transcript (475nt) containing 121 amino acid (aa) open reading frame (Figure 2B-ORF). The northern blot performed on a series of RNA extracted from embryonic (Figure 2C) and 3 weeks old mouse tissues (Figure 2D) revealed that *Smpec* transcript is restricted to the limbs and long bones. These results suggest that *Smpec* expression is restricted to chondrocytes, as there was no transcript detected from the calvaria. Subsequently, in situ hybridization was performed on mouse E16.5 tibia with probes for *Smpec* (Figure 3-left), *Col2a1*

(Figure 3-middle) and *Col10a1* (Figure 3-right) in order to find out which zones of growth plate chondrocytes express *Smpec*. *Smpec* expression was similar to *Col2a1* which was expressed in the resting and proliferating chondrocytes but not in the hypertrophic chondrocytes. The SMPEC protein is well conserved across 20 different species including mammals, birds, amphibians and reptiles. The suggested topology for the protein is a single pass transmembrane protein, having a signal peptide at the N-terminal and a transmembrane domain at the C-terminal (Figure 4B). There is no known motifs except one putative O-linked glycosylation (Ψ) and phosphorylation (*) sites (Figure 4A). In order to detect endogenous SMPEC, an antibody was raised in a rabbit against a peptide having the highest immunogenicity (Figure 4A – orange bar). After some unsuccessful trials to detect SMPEC in ATDC5 cell extracts by western blotting, it was realized that the peptide sequence chosen is covering an acceptor serine residue (serine 44 (S44)) for GAG chain addition (Figure 4A). In order to verify this, ATDC5 cells overexpressing mouse SMPEC tagged at its C-terminus with a 3xFLAG epitope (SMPEC-3XFLAG) were generated. The cells were treated with various bacterial enzymes that can selectively remove the GAG chain depending on its composition. Subsequently, western blotting with the anti-FLAG antibody was performed. The SMPEC migrated on SDS-PAGE gels as a smear with an apparent molecular mass between 35 and 60kDa (Figure 5, brackets). After treatment of live cells with chondroitinase ABC (chABC), chondroitinase ACI (chACI), or chondroitinase ACII (chACII), the smear mostly disappeared and revealed a major band at ~30kDa (Figure 5, arrowhead). All three enzymes can only

cleave and release CS sugars, and no HS nor DS. On the other hand, chondroitinase B (chB) treatment, which specifically cleaves DS, affected the migration profile only minimally, indicating the presence of a low content of DS.

There was no published information on SMPEC when this project began, but in 2011, two papers were published. One of them characterizes the expression of *Smpec* (named *Snorc*) in mice with results very similar to ours (147). The other paper studied the changes in gene expression levels in a mouse model of Temporomandibular joint osteoarthritis (TMJ-OA) using microarray. The TMJ-OA mice were generated through double KO of *biglycan* and *fibromodulin* genes. In the TMJ-OA KO mice, *Smpec* was down-regulated by 2.8 fold changes without any further details (148). There is no published literature to date describing the in vivo role of *Smpec*.

Prior to the start of my project, a global *Smpec* KO mouse was generated in order to elucidate the role of SMPEC in skeletogenesis in vivo. The targeting vector contained homology arms covering most of the promoter region (5kb) including the natural ATG (5') and a 3.5kb region encompassing the 3' untranslated region (UTR). A nuclear localization signal (NLS)-Lac-Z cassette was inserted immediately downstream of the start codon of the *Smpec* gene deleting all the 3 exons as depicted in Figure 6A. Germ line transmission in offsprings of *Smpec* chimeric males to C57BL/6 females was determined by Southern (Figure 6B) from tail clip genomic DNA (gDNA) as described by Ito et al. (149) using DNA restriction enzyme *Spe*I. After hybridization, as expected from the normal and targeted alleles, a single DNA product with a size of 12.7kb for the WT, a single DNA product with a size of 6.9kb

for the KO and both bands for the heterozygous were detected. Northern blotting performed on RNA extracted from femur epiphysis indicated that no *Smpec* transcripts were produced in the KO (Figure 6C). Western blotting performed from rib cages at 4 days post natal (P4) also confirmed the total absence of SMPEC protein (Figure 6D).

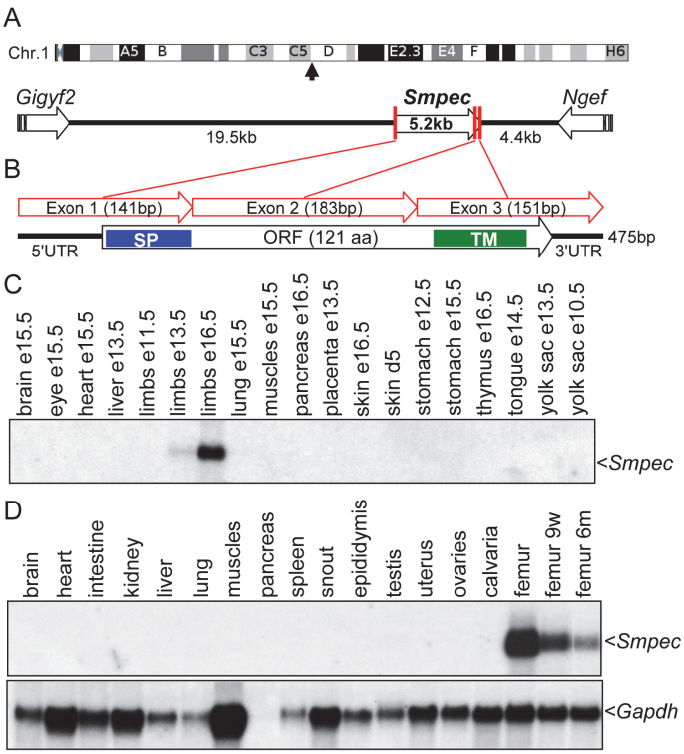

Figure 2: *Smpec* gene location and its expression in mouse tissues. (A) The *Smpec* gene is located in chromosome 1 in mice.(B) The *Smpec* gene spans 5.2kb, composed of three exons and coding for 121 amino acids in mice. (C) The mRNA expression using northern blot of different mouse tissues at different embryonic stages. The expression is restricted at the limbs starting at age E13.5 with higher intensity at E16.5. (D) Northern blot of different mouse tissues at 3 weeks old and femur of 9 weeks and 6 months. The expression is restricted to the femur with lower intensity with increased age of the mouse.

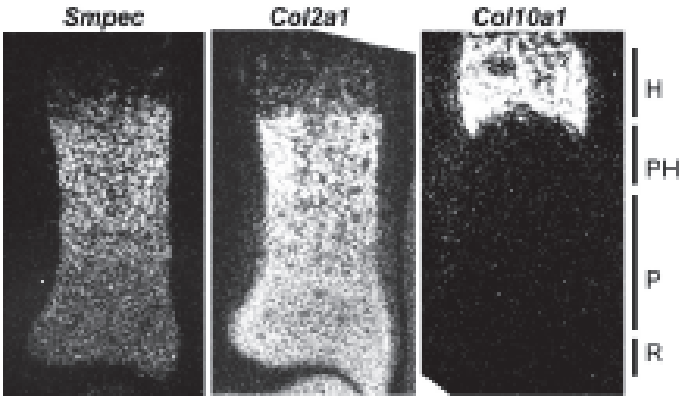

Figure 3: In situ hybridization in mouse E16.5 tibia. The mouse E16.5 tibia was probed with anti *Smpec* (left) in parallel with anti *Col2a1* (middle) and anti *Col10a1* (right). For *Col2a1* it is known that it is expressed in the resting, proliferating, and prehypertrophic zone whereas the *Col10a1* expressed only in the hypertrophic zone. *Smpec* has an expression similar to *Col2a1*.

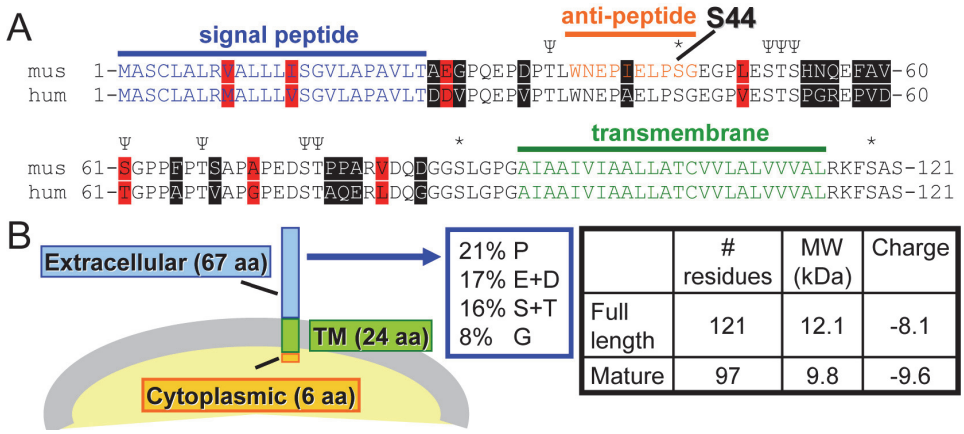

	# residues	MW (kDa)	Charge
Full length	121	12.1	-8.1
Mature	97	9.8	-9.6

Figure 4: SMPEC protein sequence and its topological prediction. (A) Sequence conservation between mouse and human respectively. The blue bar represents the signal peptide, orange bar represents the region where the rabbit anti SMPEC was raised to detect the endogenous protein and the green bar represents the transmembrane part of the protein. (B) The predicted topology for the SMPEC protein suggests it is a single pass transmembrane protein of the chondrocyte cells with N-terminal facing the extracelluar and C-terminal facing the cytoplasm.

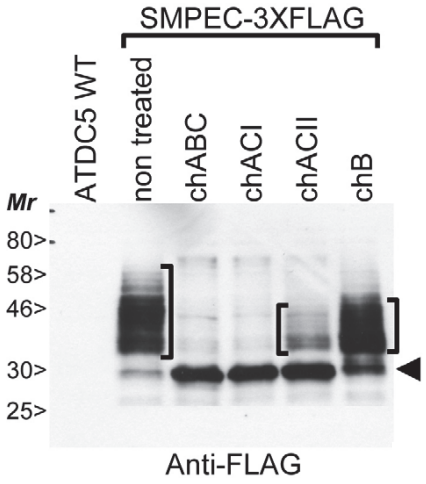

Figure 5: SMPEC is a chondroitin sulfate proteoglycan. ATDC5 cells overexpressing mouse SMPEC tagged at its C-terminus with the 3xFLAG epitope were generated. The cells were treated with either chABC, chACI, chACII or chB that can selectively remove the GAG chain then western blotting with the anti-FLAG antibody was performed. For the non treated cells, the SMPEC migrated on SDS-PAGE gels as a smear with an apparent molecular mass between 35 and 60kDa (brackets). After treatment of live cells with chABC, chACI, or chACII which release CS sugars, the smear mostly disappeared and revealed a major band at ~30kDa (arrowhead). Alternatively, chB treatment specifically cleaves DS and affected the migration profile only minimally indicating the presence of a low content of DS.

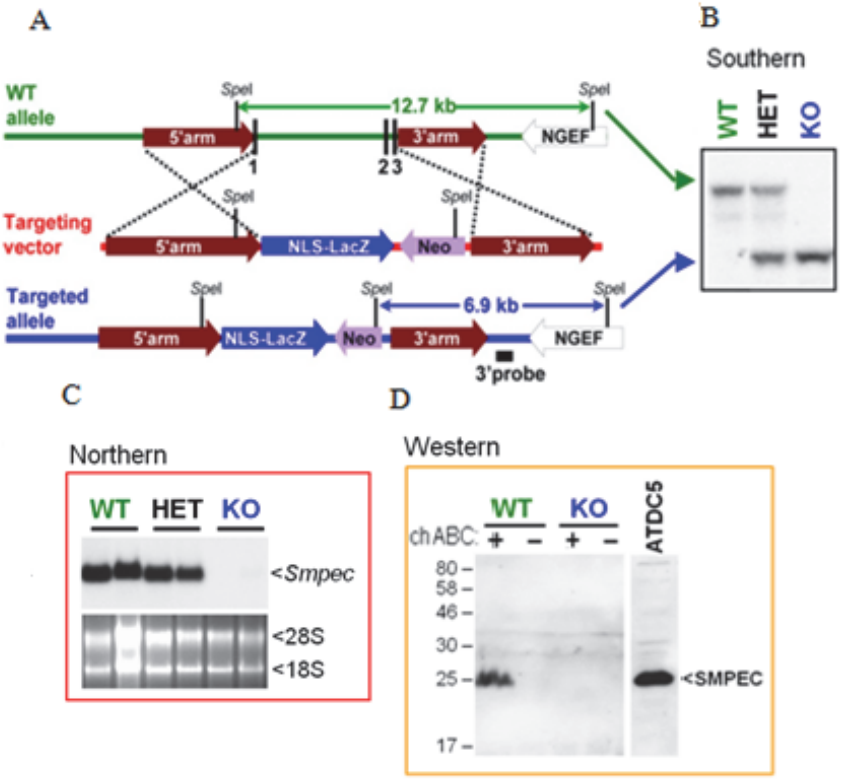

Figure 6: Generation of the *Smpec* KO mice and genotype validation. (A) Generation of global *Smpec* KO mice in which the *Smpec* gene was replaced by nuclear localization signal *lac-Z* gene. (B) Validation of the genotype of the mice through southern blot. The WT had a single 12.7 kb DNA product, the KO had a single 6.9 kb DNA product and the heterozygous had both DNA products on the gel after probing with anti *smpec* probe. (C) Northern blot on RNA extracted from femur epiphysis. WT and heterozygous had RNA band whereas the KO did not have any band on the gel after probing with anti *smpec* probe. (D) At the protein level, western blot was performed. The WT had a single band with a size of 25 KD only after chABC treatment. The KO did not have any band irrespective of chABC treatment.

Rational and Objectives

Despite the advanced understanding of chondrogenesis and endochondral ossification processes, a lot remains unknown and more investigation is needed. At this stage, the role of SMPEC in chondrogenesis and growth plate is still unknown. In order to study the *Smpec* function in vivo, a mouse model was generated with a global *Smpec* KO by other member of our lab.

The objectives of this study were to further characterize the SMPEC protein localization, and elucidate the in vivo effects of *Smpec* loss on skeletogenesis during embryonic and postnatal growth stages.

II. Materials and methods

II.1 Genotyping of the *Smpec* KO mouse

For the F2 descendants, a PCR strategy was used for the genotyping using tail clip gDNA. The DNA extraction procedure was as described by Zangala (150) and then a PCR was performed as described by Schrickel et al. (151). For the DNA extraction, mouse tail clips were digested overnight at 50ºC with rotation in 0.5ml of Tris-NaCl-EDTA (Tris–HCl pH7.4 (50mM), NaCl (100mM), EDTA (0.1mM)) containing proteinase K (0.5mg/ml) (Fisher bioreagents). After cooling to room temperature, the tubes were centrifuged at 13000RPM for 2min. The supernatant was transferred into fresh tubes and 0.6ml isopropanol was added to precipitate the gDNA. gDNA was washed with 1ml of 70% ethanol, centrifuged, and briefly dried. The gDNA pellet was resuspended with 0.1ml Tris-EDTA buffer (Tris pH8 (10mM), EDTA (0.1mM)). Each gDNA sample (0.25ml) was used for 2 separate PCR reactions having either a WT *Smpec*-specific primer, or a *LacZ*-specific primer. A typical PCR reaction mix contained 20.5µl milli-Q H2O, 2.5µl standard taq buffer (10X) (New England biolabs), 0.5µl dNTP mix (10mM) (Invitrogen), 0.5µl forward primer (25µM), 0.5µl reverse primer (25µM), 0.25µl recombinant Taq DNA polymerase (New England biolabs). The forward primer used is located in the 5`UTR of the *Smpec* gene (5`-TGCGCGTGCATGTGTGAG-3`), and the reverse primers are either within the coding region of *Smpec* (5`-AGGACCCCAGAGATGAGC-3`), or in the *Lac-Z* gene (5`-TTCTCTTCTTCTTCGGCCGC3-`). The PCR program was as follows: one denaturation step at 94°C for 2 minutes followed by 35 cycling at 94°C

for 30 seconds; 58°C for 25 seconds; 72°C for 25 seconds. Then, the amplified DNA was loaded on 2% agarose gel. From the agarose gel electrophoresis, a single DNA product with a size of 208bp for the WT, a single DNA product with a size of 177bp for the KO and both products for the heterozygous were detected.

II.2 X-Gal Staining of embryo

WT and KO embryos E17.5 were fixed, washed, stained as described by Loughna and Henderson (152). X-Gal staining of mice allows for the monitoring of sites where the *Smpec* gene is normally expressed. WT and KO embryos E17.5 were fixed with cold lac-Z fix solution (Paraformaldehyde/phosphate buffered saline (PFA/PBS) pH7.4 (1%), EGTA (5mM), NP40 (0.2%), $MgCl_2$ (2mM), Glutaraldehyde (0.2%), PBS pH7.4) for 60 minutes at 4^oC. Embryos were transferred into lac-Z wash solution (Sodium deoxycholate (0.01%), NP40 (0.02%), $MgCl_2$ (2mM), PBS pH7.4) for wash 3 X 20 minutes at RT^o. Then, embryos were stained with X-Gal staining solution (Sodium deoxycholate (0.01%), NP40 (0.02%), $MgCl_2$ (2mM), PBS pH7.4, $K_3Fe(CN)_6$ (5mM), $K_4 Fe(CN)_6$ (5mM), X-gal in N,N-dimethyl formamide (1mg/ml)) for overnight at RT^o. Next day embryos were fixed with 4%PFA/0.1M PM for overnight at 4^oC then transferred to 30% EtOH 1X30 minutes followed by 50% EtOH 1X30 minutes. Stained embryos kept at 70% EtOH for storage.

II.3 Alcian blue/alizarin red staining

WT and KO mice at P4 were processed for alcian blue and alizarin red exactly as was previously described by McLeod (153). Newborn mice of P4 WT and KO were skinned, eviscerated, and dehydrated in 100% EtOH and acetone each for overnight

then rinsed with 70%EtOH. Skeletons were stained with Alizarin Red, Alcian Blue staining solution (1:20 dilution of 0.1% Alizarin Red (Sigma), 0.3% Alcian Blue (Sigma) in 85% EtOH/5% CH3COOH) for 7 days at RTº. Skeletons were then cleared in 1% KOH/H_2O at 37º C for 3 days then incubated with 20% glycerol in1% KOH/H_2O then to 40% glycerol in1% KOH/H_2O each for overnight at RTº and stored in 40% glycerol/H_2O. Pictures were taken under a dissecting microscope (Leica MZ6) and digital pictures were generated. All pictures were taken at exactly the same magnification. Measurements of diaphysis length, diaphysis width, epiphysis height and width were then performed using the imaging software Photoshop.

II.4 5-bromo-2'-deoxyuridine labeling

To assess proliferation, P4 WT and KO mice were injected intraperitoneally with 5-bromo-2'-deoxyuridine (BrdU) at a dose of 50µg/g body weight two hours before being sacrificed. BrdU was detected in paraffin sections using biotinylated mouse anti-BrdU antibody provided with the kit as instructed by the manufacturer (Invitrogen BrdU staining kit, Invitrogen).

II.5 Immunofluorescence on cryosections

Freshly dissected mouse long bones were fixed with 4% (w/v) PFA/PBS overnight at 4°C. The next day, bones were decalcified with immunocal (Decal Chemical Corporation) for 48 hours at 4°C, washed with distilled water, and infiltrated with 20% (w/v) sucrose in PBS for 24 hours at 4°C. Bones were embedded in sucrose:OCT (2:1) and sectioned using a cryomicrotome. Cryosections of P4 WT were fixed with 4% PFA/PBS for 10 minutes at RT°. Sections were then treated with

chABC (Tris-acetate pH7.3 (0.1M), EDTA (1mM), phenylmethylsulfonyl fluoride (PMSF) (1mM), protease inhibitor cocktail (Sigma) (1X), chABC (0.25U/ml) (Biolynx)) in a humidified chamber for 45 minutes at 37°C prior to being blocked with 5% skim milk/PBS in a humidified chamber for 1 hour at RT°. Sections were probed with primary antibody diluted in 2.5% milk/PBS for 1.5 hours at RT° in a humidified chamber followed by incubation with Alexa Fluor ® 488 goat anti-rabbit IgG (H+L) seconday antibody (1/1000) (Invitrogen) in a humidified chamber for 1 hour at RT°. Sections were mounted with prolong gold antifade with 4',6-diamidino-2-phenylindole (DAPI) (Invitrogen).

II.6 Immunohistochemistry on cryosections

Cryosections from embryonic WT E18.5 mice were fixed with 4% PFA/PBS for 10 minutes at RT°. Sections were treated with chABC as described above. Endogenous peroxidase was blocked with 0.3% H_2O_2/methanol for 30 minutes at RT°. Sections were then processed as recommended by the manufacturer (VECTASTAIN ABC Kit, Vector). Signal was detected using Vector DAB substrate kit as recommended by the manufacturer (Vector). Finally, sections were counterstained for 5 seconds at RT° with hematoxylin QS (Vector) and then mounted with microkit (Mecalab).

II.7 Immunohistochemistry on paraffin embedded sections

Freshly dissected mouse P4 long bones were fixed with 4% PFA overnight at 4°C. The next day, bones were decalcified with EDTA (15%) for 14 days at 4°C before paraffin embedding and sectioning. Sections were deparaffinised and rehydrated by

sequential treatment with 1X5 minutes xylene, 2X2 minutes xylene, 2X5 minutes 100% EtOH, 1X5 minutes 95% EtOH, 1X5 minutes 70% EtOH, 1X5 minutes 50% EtOH, 1X5 minutes 30% EtOH, 2X5 minutes H_2O then 1X5 minutes PBS. Then, sections were processed as was mentioned above for the cryosections starting with chABC treatment.

II.8 Primary antibodies

The SMPEC protein was detected with an affinity-purified rabbit anti-mouse SMPEC primary antibody, at a dilution of 1/300 (generated by other member of our group as described in the introduction). COL2A1 primary antibody is a commercial monoclonal anti-mouse (Developmental Studies Hybridoma Bank), used at a dilution of 1/50 and COL10A1 primary antibody is a polyclonal anti-mouse (154), used at a dilution of 1/150. These concentrations are for the IHC and IF procedures.

II.9 Safranin O / Fast green staining

Sections (8μm) of P4 WT and KO mice were deparaffinised in xylene followed by a graded series of alcohol washes as described above. Sections were stained with weigert iron hematoxylin 1X5 minutes then with 0.02% fast green (Sigma) for 1 minute at RT^o. Then sections were rinsed with 1% acetic acid 2X10 seconds followed by staining with 0.1% Safranin-O (Sigma) 1X5 minutes. Stained sections were washed with distilled water then mounted with microkit (Mecalab).

II.10 Primary chondrocyte cultures

Primary chondrocytes were prepared from rib cages of P4 neonatal WT and KO mice in which all bony parts were first carefully removed under a dissecting

microscope. The procedure was adapted from Gosset et al. (155). Rib cages were rinsed in sterile PBS, and incubated in a petri dish for 90 minutes at 37°C with a mixture of collagenase D (3mg/ml) (Roche) and Trypsin (0.1%) (Invitrogen) dissolved in digestion media, with vigorous mixing every 30 minutes. The digestion media consisted of DMEM:F12 (Invitrogen) supplemented with 100U/ml penicillin and 100µg/ml streptomycin. After this initial digestion, the loosened ribs were decanted and the supernatant with liberated cells was discarded. The ribs were digested further with collagenase D (3mg/ml) in digestion media for 3 hours at 37°C with mixing vigorously every hour. Again the ribs were decanted and the supernatant discarded. The ribs were finally digested with collagenase D (0.67mg/ml) in digestion media overnight at 37°C. The next morning, after vigorous shaking and filtration, cells were counted with a hemacytometer and seeded at a density of 130,000 cells/well in 12 wells plates. The cells were cultured in DMEM:F12 (1:1) supplemented with 10% (vol/vol) fetal bovine serum (FBS) (Invitrogen), 100U/ml penicillin and 100µg/ml streptomycin. Cells were incubated at 37 °C in 5% CO_2 and media replaced three times per week. Upon confluence (referred to as day 0), 50µg/ml ascorbic acid was added to the media. Cells were collected at three different time points (day 0, 7 and 14).

II.11 RNA isolation and Quantitative Real-Time Polymerase Chain Reaction (RT-qPCR) from cartilage

Freshly dissected WT and KO at P4, P28 and 12 months articular cartilage and femur condyles were pooled and homogenized with a Polytron (Kinematica Polytron) in TRIzol (Invitrogen). Purified mRNA was suspended in 10µl DEPC-treated H_2O

and quantified using a NanoDrop. mRNA was diluted (2µg in 10µl DEPC-treated H_2O) then reverse-transcribed to cDNA using the High-Capacity cDNA Reverse Transcription Kit (Applied Biosystem). The obtained cDNAs were used for real-time qPCR reactions in a 96-well plate (at 100ng/well) and mixed with PCR Universal Master Mix (Applied Biosystems), gene specific TaqMan probe, and DEPC-treated H_2O in 25µl reactions. The 96-well plate was then placed in a 7500 Real Time PCR system (Applied Biosystems) for qPCR analysis. Gene expression of *Smpec, opn, Tnap, Prg4, Ank, Enpp-1, Mgp* and *Acan* was then assessed by RT-qPCR using the ΔCt method. Equal cDNA concentration and total volume was loaded in all wells in triplicate. Data was normalized to β-actin mRNA levels.

II.12 RNA isolation and Quantitative Real-Time Polymerase Chain Reaction (RT-qPCR) from chondrocyte cultures

Chondrocyte cultures were washed three times with PBS, and collected with 1mL TRIzol Reagent (Invitrogen). Total RNA was extracted, quantified and reverse transcribed as above. Gene expression of *Col2a1, Col10a1, Acan, Sox9* and *Smpec* was then assessed by RT-qPCR and data was normalized to β-actin mRNA levels and analyzed as above.

II.13 Alcian blue staining of chondrocyte cultures

Cells of WT and KO mice were washed with PBS and fixed with 100% cold methanol for 30 minutes at 4^{o}C. Cells were incubated with alcian blue pH1.0 (0.3%) (Sigma) overnight at RT^{o}. The next day, cells were washed extensively with distilled water and the dye was extracted with 500µl guanidine-HCl (6M). The solubilized alcian blue dye was loaded into a 96-well plate at 200µl/well which was then placed in an EL 808 spectrophotometer (Bioteck) for quantitative analysis. The dye has a maximum absorbance at 630nm. A standard curve of alcian blue prepared in guanidine-HCl (6M) was plotted to normalize the samples to it.

II.14 Imaging and statistical analysis

All images were captured with an Olympus DP-70 camera connected to a Leica DMR microscope. All the images were analyzed using DP Controller software. Results are expressed as mean ± SEM for all counts. Statistical analysis was evaluated by two-tailed Student's t-test. $P < 0.05$ was considered statistically significant.

III. Results

III.1 Characterization of SMPEC expression and co-localization in vivo

Immunohistochemistry (IHC) on cryosections from embryonic WT E18.5 mice was performed to explore the expression pattern of SMPEC in vivo. The signal obtained indicated that SMPEC is expressed in all cartilaginous elements including nasal septum (Figure 7A), Meckel cartilage of the jaw bones (Figure 7B), clavicle and cricoid cartilage (Figure 7C), vertebra (Figure 7D and H), ribs (Figure 7E) and hind limb (Figure 7G). SMPEC was not detected in any other tissues and the lung is shown magnified as a representative example (Figure 7F).

To explore its expression at a later age and co-localization, immunofluorescence (IF) against SPMEC was performed on paraffin embedded distal femur of P4 WT mice, in parallel with COL2A1 and COL10A1 (Figure 8). COL2A1 (Figure 8A', B' and C') was detected in the ECM of all zones, and COL10A1 (Figure 8A", B" and C") was restricted to the ECM of the hypertrophic zone only. SMPEC labeling was found associated with the cell membrane of the resting and proliferating chondrocytes (Figure 8A and B) and the ECM of the hypertrophic chondrocytes (Figure 8C). More specifically, SMPEC immunoreactive signal was quite strong in the intercolumnar septum of the hyperthrophic chondrocytes, suggesting that it is shed from the cell surface (Figure 8C). In order to validate the specificity of the anti-SMPEC antibody used, IHC on paraffin sections from the distal femur of P4 WT and KO mice was performed (Figure 9). The immunostaining in the WT distal femur was as observed for the IF staining, where the signal obtained was mostly over proliferating and pre-hypertrophic chondrocytes (Figure 9- left). Absolutely no SMPEC signal was detected on tissue sections from KO mice (Figure 9- right) indicating that the anti-SMPEC antibody used is highly specific and does not generate any background.

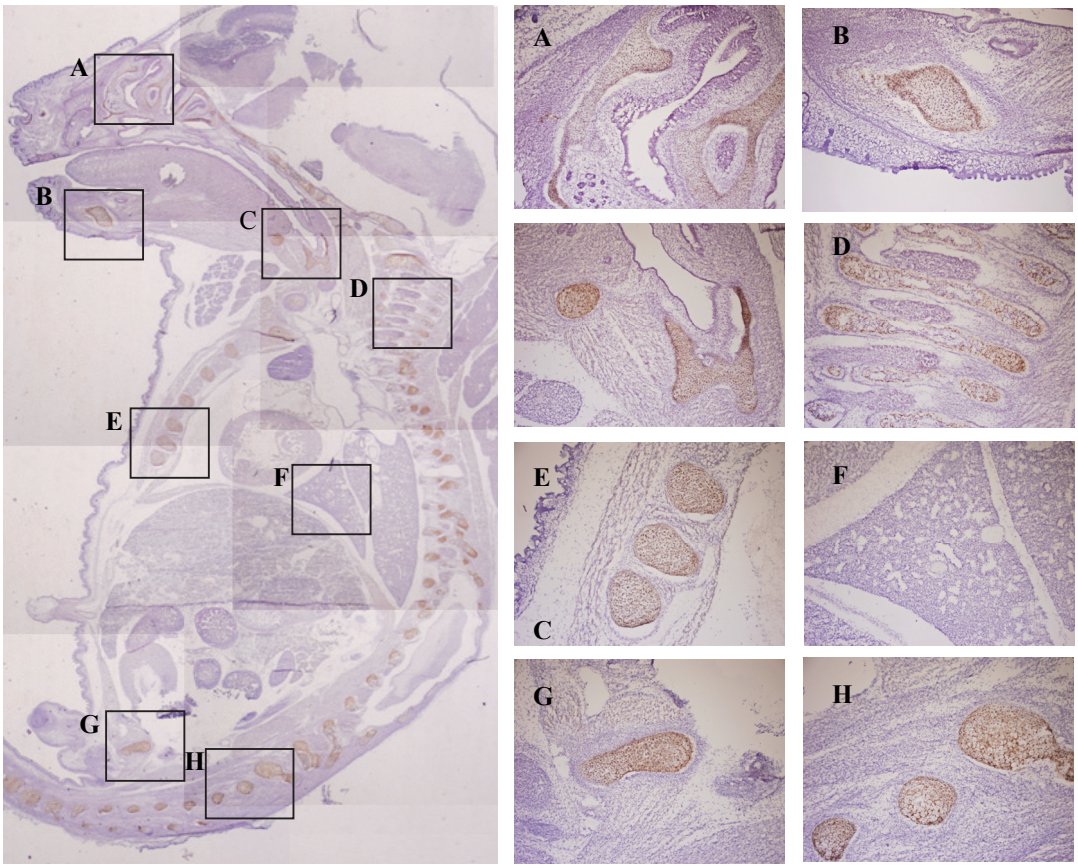

Figure 7: Endogenous expression of SMPEC protein on embryo E18.5 mouse tissue. IHC with rabbit anti SMPEC antibody after chABC treatment performed on E18.5 WT mouse. Tissues boxed are nasal septum (A), Meckel cartilage of the jaw bones (B), clavicle and cricoid cartilage (C), vertebra (D and H), ribs (E) lungs (F) and hind limb (G). The SMPEC expression (brown color) was restricted on chondrocytic sites including tissues A through H except the lung (F) which selected as an internal negative control. Picture at 2.5X on left and at higher magnification10x on right (n=8). The section was counterstained with hematoxylin (blue color).

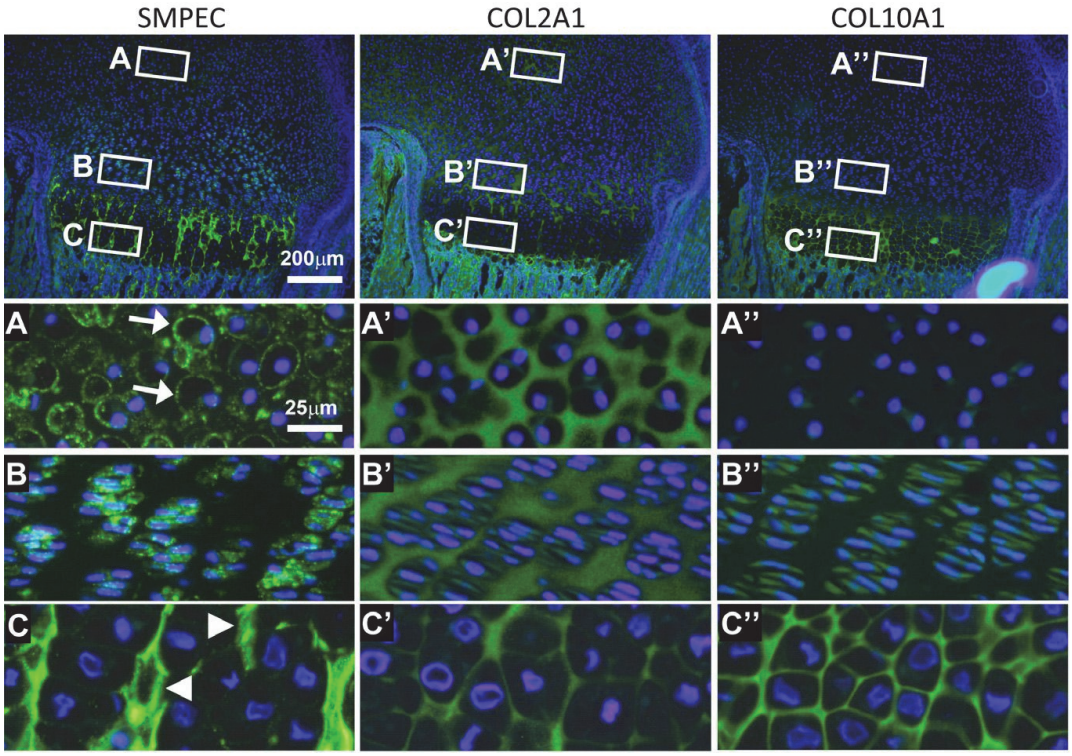

Figure 8: Immunofluorescence localization of SMPEC, COL2A1 and COL10A1 in mouse P4 distal femur. The mouse P4 distal femur (n=5) was probed with anti SMPEC (left) in parallel with anti COL2A1 (middle) and COL10A1 (right). The zones are resting (A, A' and A"), proliferating (B, B' and B") and hypertrophic (C, C' and C''). For SMPEC, the protein was detected (green color) in all the zones (A, B and C). For resting and proliferating zone, SMPEC was detected on the plasma membrane (A and B) whereas at the hypertrophic zone, the signal was detected in the intercolumnar septum (arrow head in C) in which *Smpec* gene is not expressed. This suggests that the protein is shed off in the transition of prehypertophic zone to hypertrophic chondrocytes. For the COL2A1 the protein was detected in the ECM of almost all zones (A', B' and C'). whereas COL10A1 was detected in the ECM of the hypertrophic zone only (A", B" and C''). Sections were counterstained with DAPI (blue color).

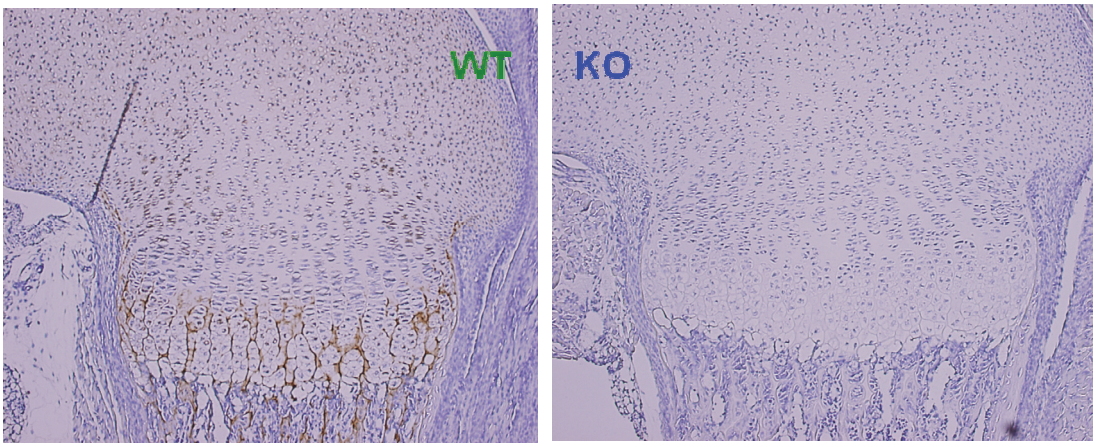

Figure 9: Endogenous expression of SMPEC protein on P4 mouse distal femur. IHC with rabbit anti SMPEC antibody after chABC treatment performed on P4 WT and KO mouse respectively. In the WT section, SMPEC detected in the resting, proliferating as well as in the hypertrophic zone in the intercoloumnar septum (brown color) (left) as was seen in the IF. No signal was detected in KO section (right). Picture taken at 10x (n=7 of each group). Sections were counterstained with hematoxylin (blue color).

III.2 Characterization of *Smpec* KO mice

In order to elucidate the role of SMPEC in skeletogenesis in vivo, a mouse model was generated by other member of our group in which the *Smpec* gene was ablated and a nuclear localization signal (NLS)-Lac-Z cassette was inserted immediately downstream and in frame with the natural start codon of the *Smpec* gene (Figure 6A). The functionality of the *Lac-Z* cassette to mimic endogenous *Smpec* expression was tested by whole mount X-gal staining performed on E17.5 WT and KO mice. In KO mice a signal was detected at the ribs, limbs and mandible (Figure 10A- right). For WT, only pale non-specific back ground was detected (Figure 10A-left). This indicated that the lac-Z reporter recapiluted *Smpec* expression. Lastly, genotyping PCR using mouse tail DNA was established from the F2 descendants. As determined by agarose gel electrophoresis a product of 208bp was detected for the WT allele (Figure 10B- middle), and a product of 177bp was detected for the KO allele (Figure 10B- right). For heterozygote, both were detected (Figure 10B- left).

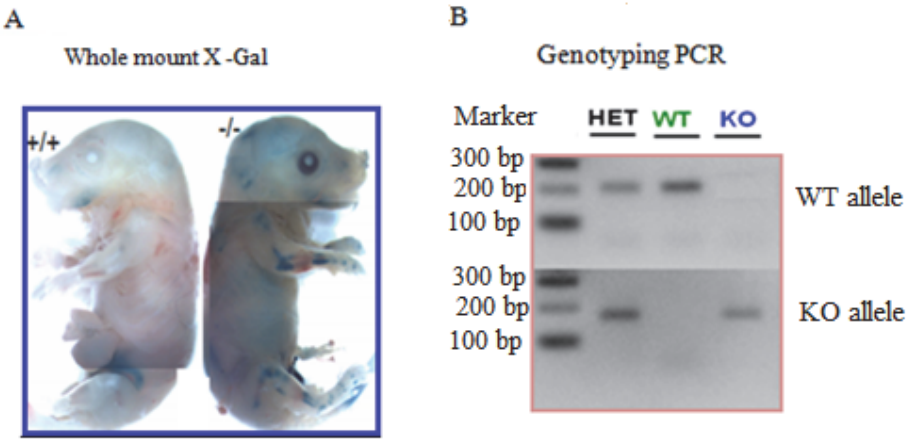

Figure 10: Genotype validation. (A) Whole mount-X gal staining in which the *Lac-Z* expression mimics that of *smpec*. Specific signals were detected in the KO only. (B) Genotyping PCR using a mouse tail DNA. After gel electrophoresis, the WT had a single DNA band with a size of 208bp, the KO had a single DNA band with a size of 177bp and heterozygous had both DNA bands.

III.3 Alcian blue/alizarin red skeletal staining

The KO mice were fertile and developed normally, at least by visual whole-body examination. In order to more precisely assess whether changes in cartilage and bone were present, whole-mount skeletal staining with alcian blue/alizarin red which stains cartilage and bone, respectively, was performed on the arms P4 KO and WT. There was no obvious gross qualitative changes in the relative intensities of staining for both dyes in the P4 KO versus WT (Figure 11A), and apparently no patterning defects. Thus, more precise measurements of the diaphysis length, diaphysis width, epiphysis height and epiphysis width were performed on the humeri. Upon analysis, the diaphysis of KO mice was 6.6% shorter than WT and epiphysis height and width were reduced by 8.3% and 12.4% respectively. However, there was no significant difference in the diaphysis width between KO and WT (Figure 11B). This indicated that the longitudinal growth was reduced by the lack of SMPEC and as all long bones developed by the same mechanism, we hypothesized that the longitudinal growth of all long bones reduced by the lack of SMPEC.

III.4 Epiphyseal growth plate analysis

Having established that the *Smpec* KO long bones are shorter than the WT, we went into more refined measurements on tissue sections specifically focusing at the growth plate. Safranin O/Fast Green staining which stains the PG deposit in the ECM was performed on a section of P4 whole leg neonatal WT and KO mice. There was no significant difference in the PG deposition between KO (Figure 12A-right) and WT (Figure 12A-left). Histological analysis demonstrated that femurs of P4 *Smpec* KO appeared to have lower cellularity in the resting (Figure 12A-top right and left) and the proliferating (Figure 12A-middle right and left) zones. Quantitative analysis confirmed the significant reduction in the cell number in the resting zone of the KO mice compared to WT (Figure 12B). However, the columnar organization in the

proliferating zone seemed to be normal in the KO compared to WT (Figure12 A-middle right and left). The hypertrophic zone also appeared not to be altered (Figure 12A-bottom right and left). Because the most important contributor for the longitudinal growth of long bones is chondrocyte hyperthrophy, quantitative analysis was performed. This was achieved through IHC on P4 distal femur using an antibody against COL10A1, a marker of hypertrophy (Figure 13A). Measurements of the hypertrophic COL10A1 positive zone thickness indicated no statistically significant difference between the KO and the WT (Figure 13B). Next, we investigated whether the lack of SMPEC could have affected the proliferation rate and/ or cell count in the proliferating zone. This was achieved by IHC using antibody against BrdU (Figure 14A), which was administered two hours before tissue collection. BrdU is a nucleotide analog that incorporates into newly synthesized DNA and is thus a surrogate marker of proliferation. This ensure that we can determine the border of the proliferating zone more precisely thus the quantification analysis of the total numbers of cells in this zone will be more accurate. Quantitative analysis of the BrdU IHC demonstrated that KO mice have normal chondrocyte proliferation, as displayed by a similar percentage of positive cells between the WT and KO mice (Figure 14B-top). There was a statistically significant reduction in the total numbers of cells /μm^2 in the KO proliferating zone compared to the WT (Figure 14B -bottom).

A

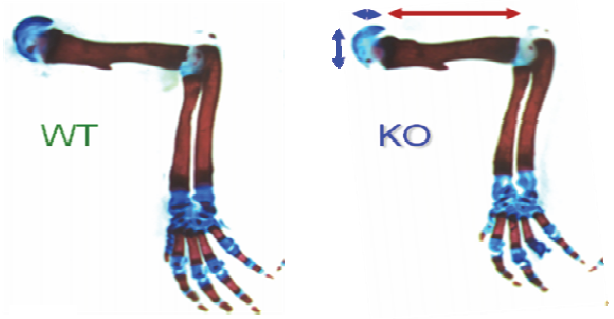

B

Means ± SEM	WT (n=19)	KO (n=26)	t test P-value	%reduction
Diaphysis length (mm)	4.07 ± 0.09	3.80 ± 0.08	0.03	6.6
Diaphysis width (mm)	0.66 ± 0.01	0.63 ± 0.02	0.17	ns
Epiphysis height (mm)	0.96± 0.03	0.88 ± 0.02	0.02	8.3
Epiphysis width (mm)	1.53 ± 0.05	1.34 ± 0.04	0.003	12.4
Total length (mm)	5.687 ± 0.12	5.097 ± 0.18	0.02	10.4

Figure 11: Lack of *Smpec* results in reduced growth of P4 mice long bones. (A) staining of the P4 mice arm of WT and KO with alcian blue/alizarin red staining. The stain intensity was similar comparing the KO with the WT. (B) Statistical analysis after measuring the bones of the two groups revealed a significant reduction in the KO (n=26) diaphysis length, epiphysis height and width but not in the diaphysis width compared to the WT (n=19). $P < 0.05$.

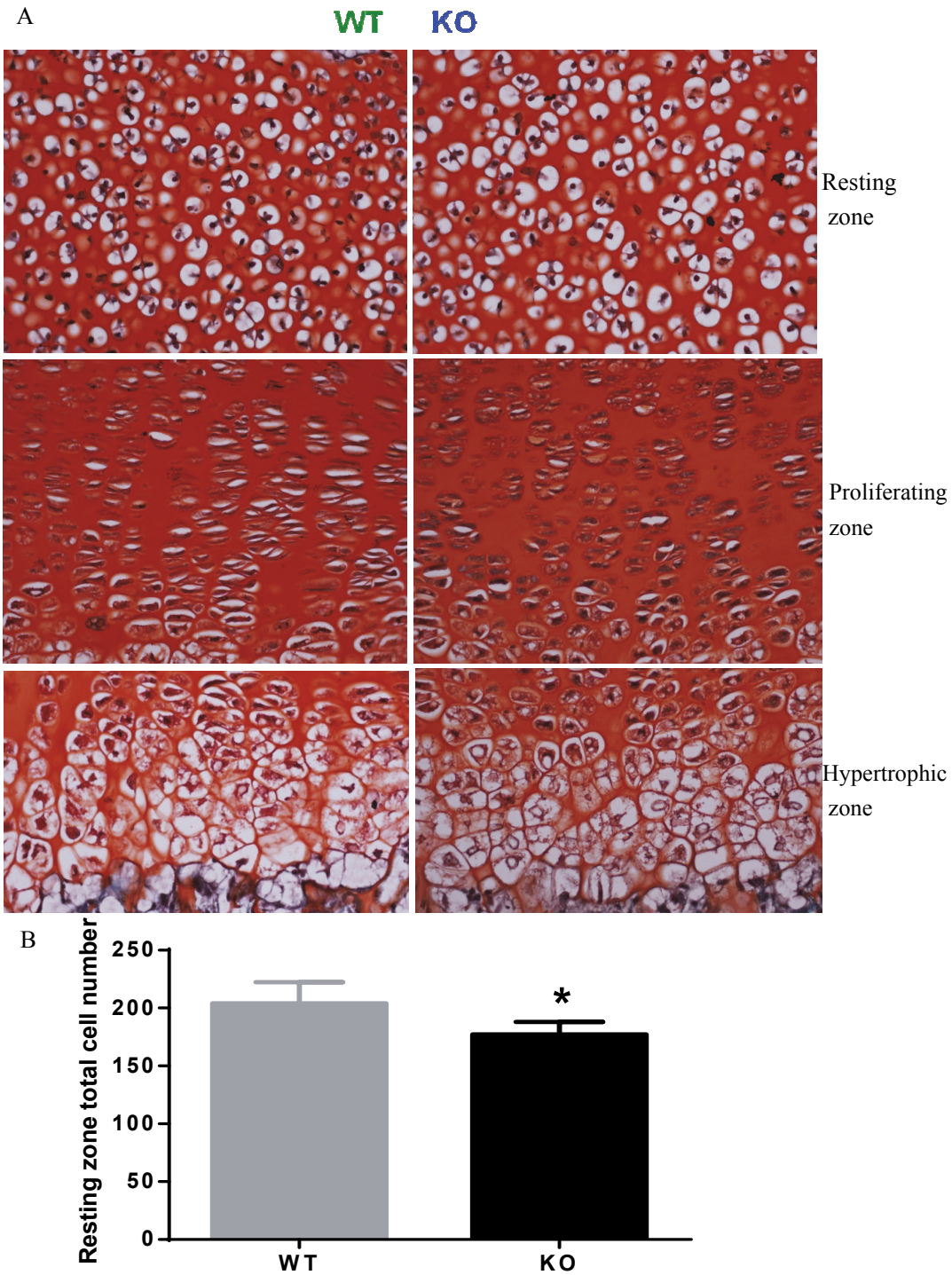

Figure 12: Histological analysis with Safranin O/Fast green P4 distal femur. (A) Indicates the different zones of the growth plate after staining with Safranin O/Fast green which stains PG (red color). The intensity of the stain was similar between the KO (n=7) and the WT (n=5) taken at 40x. This indicates that PG deposition is not affected by *Smpec* ablation. On the other hand, the cell number seems to be less in the resting as well as the proliferating zones in the KO compared with the WT. The hypertrophic zone seems to be normal. Sections were counterstained with hematoxylin (blue color) (B) Statistical analysis showed a significant reduction in the KO resting zone total cell number compared to the WT.*P < 0.05.

A

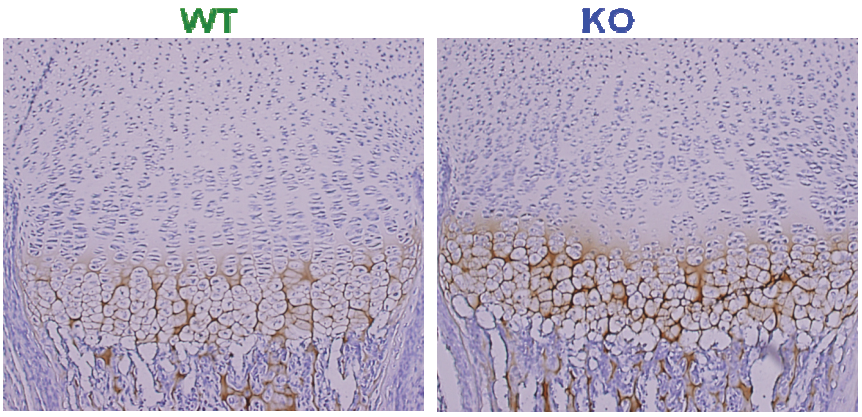

B

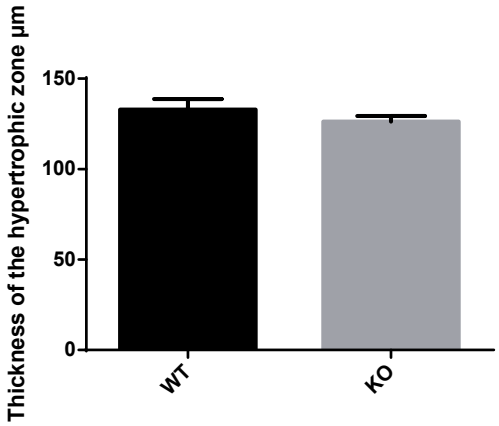

Figure 13: Immunohistochemistry labeled with COL10A1 of P4 distal femur. (A) Representative figure of the P4 distal femur labeled with COL10A which specifically labeled the hypertrophic zone (brown color) taken at 10x. The section was counterstained with hematoxylin (blue color). (B) Measurements of the labeled hypertrophic zone indicated no significant difference between the KO and the WT (n= 4 and 7 respectively).

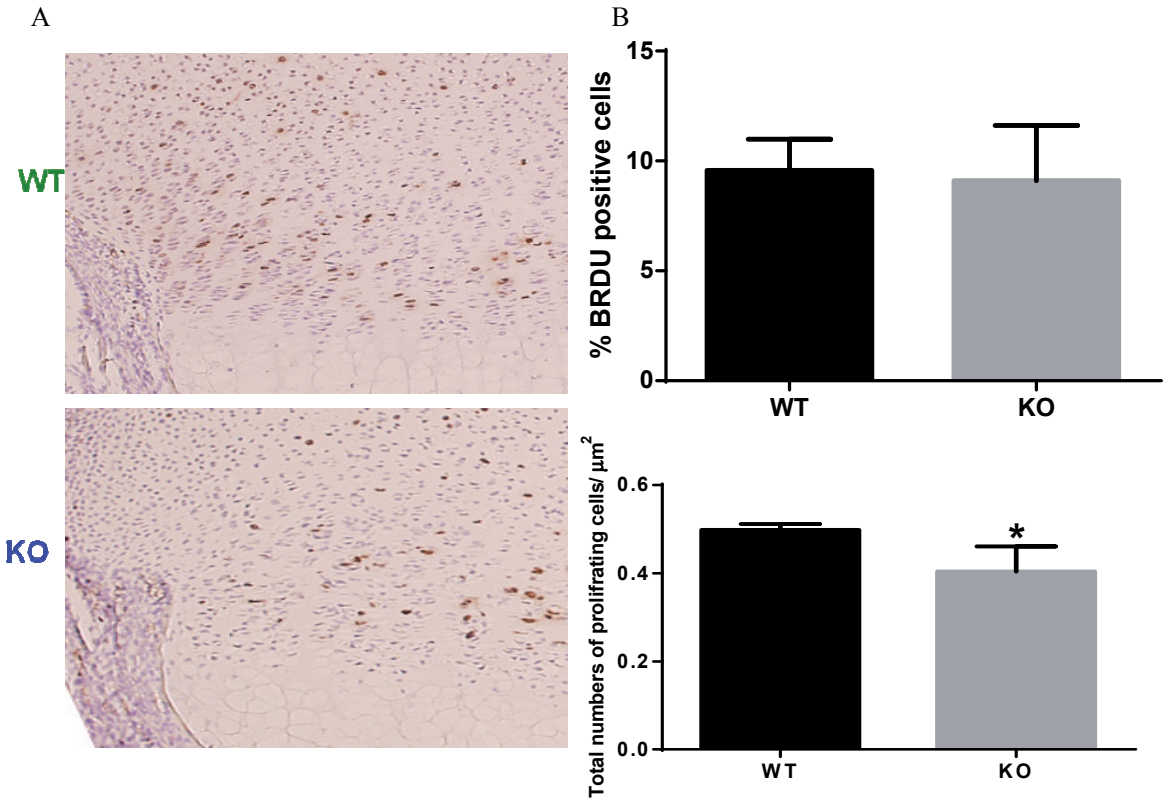

Figure 14: Immunohistochemistry labeled with Brdu of P4 distal femur. (A) The labeling with Brdu (brown color) of the WT and KO respectively of P4 growth plate mice taken at 10x. Sections were counterstained with hematoxylin (blue color). (B) Statistical analysis to determine the effect of *Smpec* loss on the rate of proliferation and the total number of cells in the proliferating zone. For the proliferation rate, there was no significant difference between the KO and the WT (B-top). Whereas the total number of cells in that zone was significantly reduced in the KO compared to WT (B-buttom). (n=5 of each group).*$P < 0.05$.

III.5 Expression profile of selected genes important for growth plate function, skeletogenesis and mineralization

In order to investigate at the molecular level whether gene expression patterns were affected in the KO mice, RNA was extracted from femur condyle and articular cartilage of P4, P28 and 12 month old WT and KO mice. Real-Time qPCR was performed on *Smpec* as well as on a selected set of genes known to be expressed in chondrocytes and are important for mineralization (*Opn, Tnap, Prg4, Ank, Enpp-1, Mgp* and *Acan)*. These genes were selected based on a previous in vitro study on ATDC5 chondrocytes, performed by one of our group member, indicating that *Smpec* knockdown favoured mineral deposition as revealed by alizarin red staining (unpublished). Confirming the genotype of the mice used, *Smpec* was absent in all of the three tested ages of the KO (Figure 15). However, none of the genes monitored displayed reproducible and consistent changes in the three age time-points. Only subtle and transient significant changes were observed. Also, variance analysis on groups of mice often showed unequal distribution that prevented us from performing a unified statistical test (Figure 15).

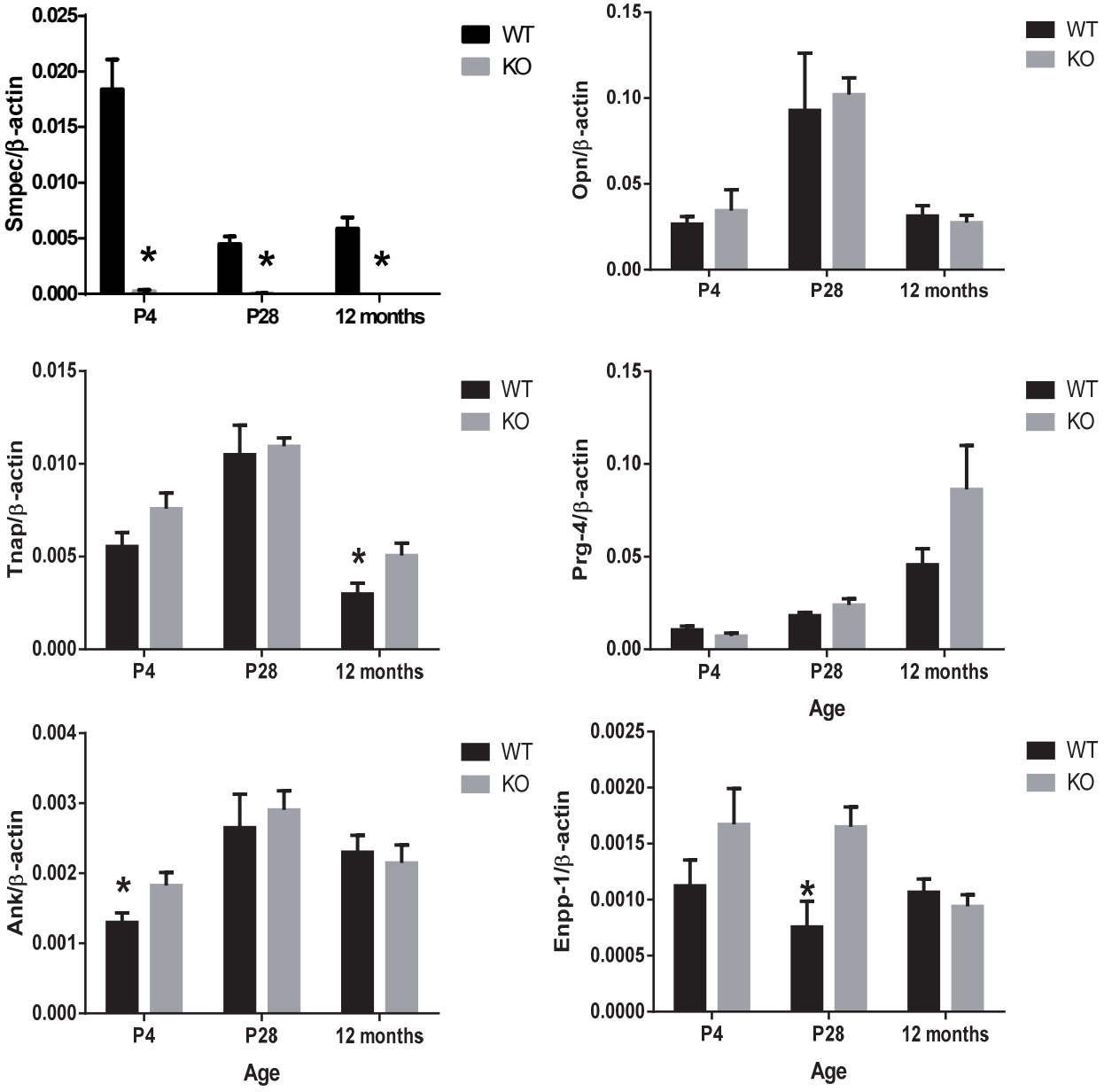
Smpec/β-actin
0.025
0.020
0.015
0.010
0.005
0.000
P4
P28
12 months
WT
KO
*
Opn/β-actin
0.15
0.10
0.05
0.00
Tnap/β-actin
Prg-4/β-actin
Ank/β-actin
0.004
0.003
0.002
0.001
Enpp-1/β-actin
0.0025
0.0020
0.0015
0.0010
0.0005
0.0000
Age

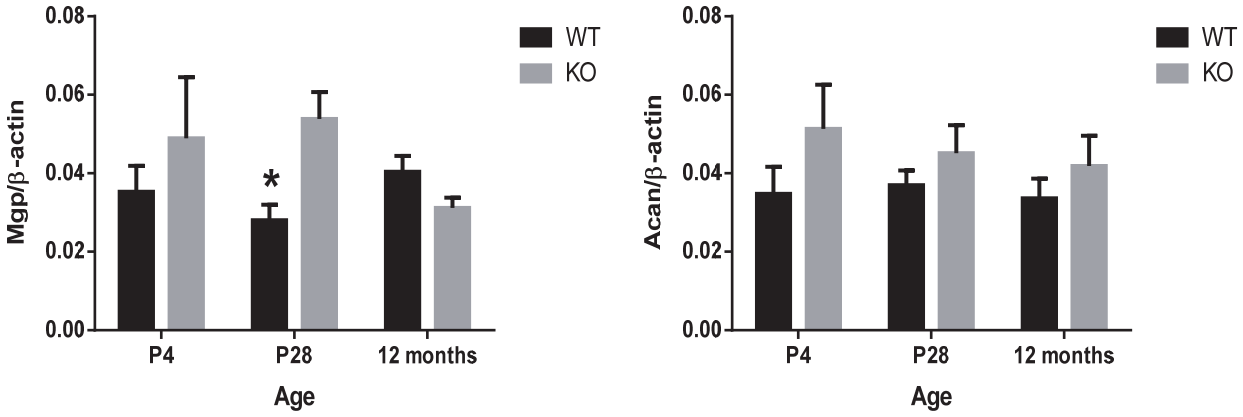

Figure 15: Expression profile of certain bone and cartilage markers. The tested genes were *Smpec*, *opn, Tnap Prg4*, *Ank, Enpp-1*, *Mgp* and *Acan*. After normalization of these genes with β-actin the expression was graphed at the tested ages P4, P28 and 12 months old. Only *Smpec* was significantly reduced in the KO compared to the WT at all ages. For *Tnap*, only significantly elevated at 12 months in the KO compared to the WT. For *Ank*, only significantly elevated at P4 in the KO compared to the WT. For *Enpp-1* and *Mgp* both were significantly elevated at P28 in the KO compared to the WT. For *Acan* there was no significant different between the two groups at all ages tested. *Opn, Tnap* and *Prg4* were excluded from the analysis due to high variances at P28, P28 and 12 months respectively. (n=6 at P4, n=5 at P28 and n=8 at 12 months. Each age was tested in triplicate for each group). * $P < 0.05$.

III.6 Primary chondrocytes cultures of P4 WT and KO

The dissection of the femur condyles and articular cartilages, although performed under a microscope, could have introduced a bias because of cell heterogeneity, and contributed to the large variance in the qPCR results. Thus, we opted to culture isolated chondrocytes from costal cartilage to be able to work with a more homogenous cell population and reduce such potential biases. Cells were monitored from day of confluence (day 0) until day14 post confluence (day 14). Representative phase contrast pictures taken from live cells revealed no striking differences in terms of morphology (Figure 16 left and right) as well as cell density in both KO and WT cultures (Figure 16 left).

III.7 Gene expression profile from the primary chondrocytes cultures

Quantitative PCR was performed in order to study the impact of *Smpec* KO on the expression of *Sox9, Col2a1, Acan* and *Col10a1* at different time points of the cultures (day 0, 7 and 14) (Figure 17). *Smpec,* as expected, was absent from KO cultures (Figure 17A). For *Sox9, Col2a1, Col10a1*, and *Acan* (Figure 17), the expression decreased with time in both cultures. Statistically there was no significant difference between the WT and KO cultures in any of those genes at any time point tested. Thus, lack of *Smpec* did not seem to affect the expression of all genes tested.

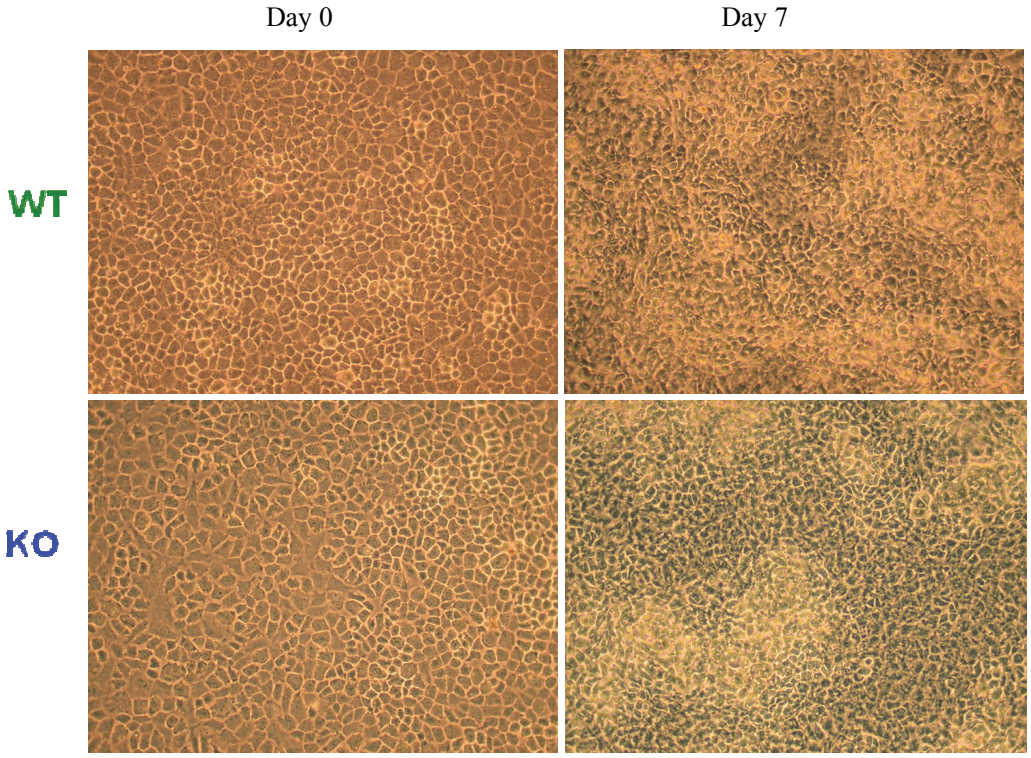

Figure 16: Primary chondrocytes cultures from costal cartilage of P4 mice. The cultures were seeded at 130,000 cells/well. Both WT and KO cultures reach confluence after 96 hours of seeding and this was designated as day 0. There was no noticeable morphological difference between the cultures of the WT and the KO which was monitored until day 14. For simplicity only one figure from each group at day 0 and day 7 is presented taken at 100X. (n=3 for each group).

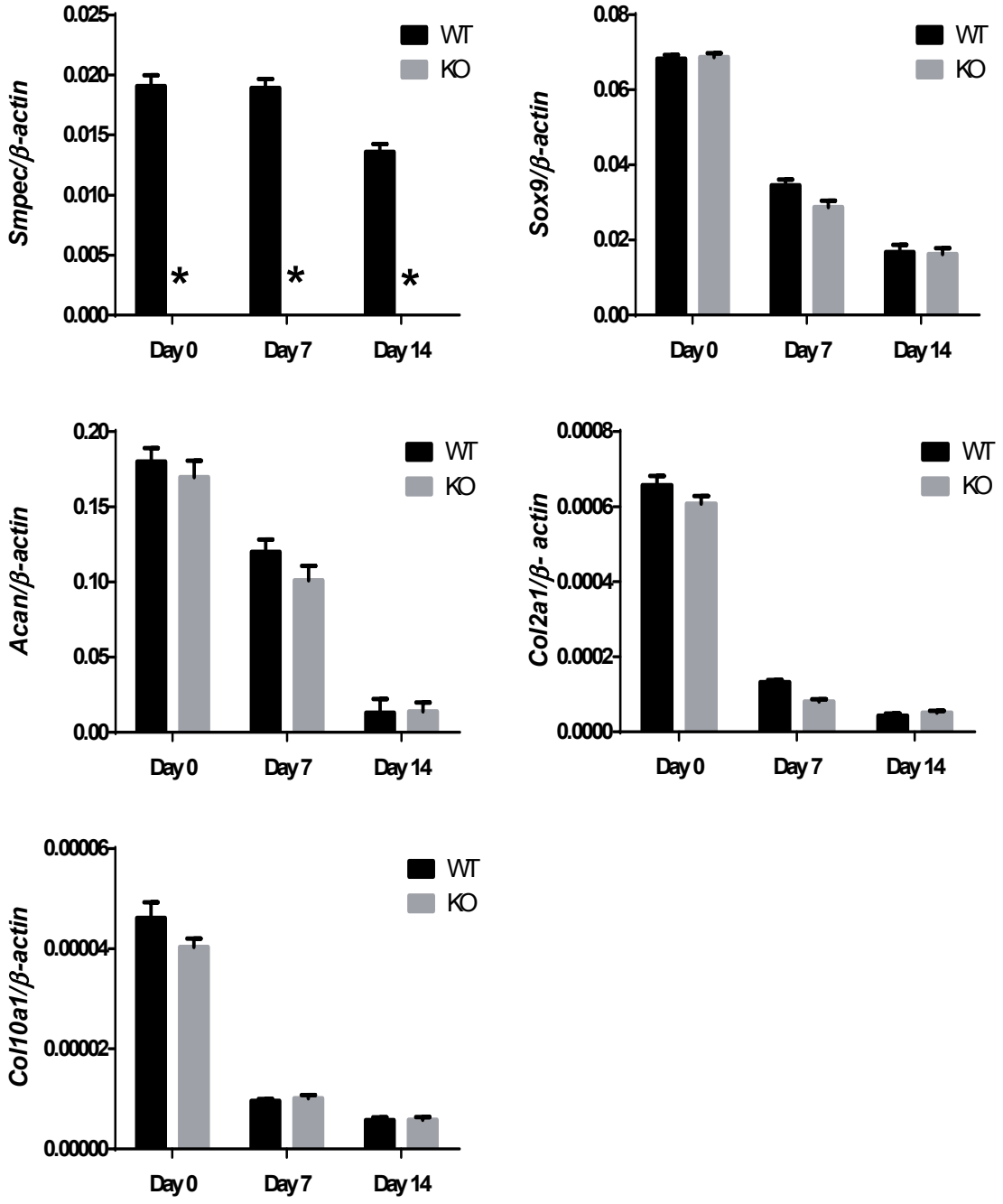

Figure 17: Lack of *Smpec* had no impact on the expression of *Sox9, Acan, Col2a1* and *Col10a1* in vitro. RNA was extracted from the costal cartilage of P4 primary mice chondrocytes cultures at day 0 (day of confluence), day 7 and day 14. The tested genes were *Smpec*, *Sox9, Acan, Col2a1* and *Col10a1*. After normalization of these genes with β-actin the expression was graphed at the tested time points day 0, day 7 and day 14. Only *Smpec* was significantly reduced in the KO compared to the WT at all time points tested. None of the other genes mentioned was significantly different between the WT and the KO. All of these genes decreased with time (n=3 at each time point and each time point was tested in triplicate for each group). * $P < 0.05$.

III.8 Metabolic activity of the primary chondrocytes in cultures

Metabolically active chondrocytes synthesize abundant matrix composed mainly of collagens, glycoproteins and PG. Alcian blue staining, which stains predominantly extracellular deposits of PG mainly ACAN, was performed at the same time points on both cultures (day 0, 7 and 14) in order to assess the metabolic activity of the chondrocytes. The staining intensity increased with time in both cultures (Figure 18A) and was qualitatively similar in the WT and KO. Quantitative measurements of the alcian blue dye after guanidine extraction revealed that although there was a slight decrease in the alcian staining in the *Smpec* KO, it was not statistically different from the WT (Figure 18B). This indicated that *Smpec* KO chondrocytes had similar capacity to synthesize, release, and deposit PG into the ECM, as compared to the WT.

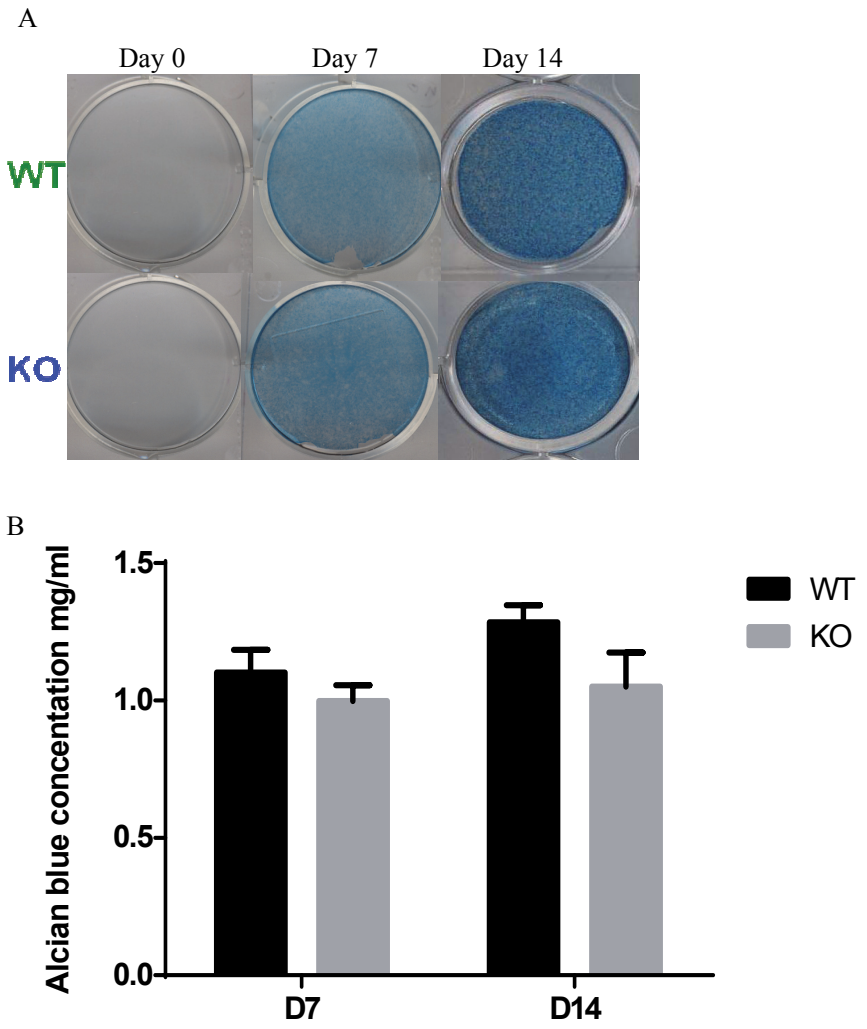

Figure 18: Absence of *Smpec* did not change the deposition of the proteoglycan ACAN in vitro. (A) Comparisons between different wells from WT and KO at different time points. For both groups the intensity of alcian blue staining which stains ACAN (blue color) increased with time with almost no stain at day of confluence (day 0) and no visual difference in the intensity at later time points between the WT and KO. (B) Quantitative analysis confirmed that *Smpec* ablation did not affect the ACAN deposition (n= 3 at each time point and each time point was tested in duplicate for each group).

IV. Discussion

Many features make the novel discovery of *Smpec* promising both in drug development and in the research field of cartilage biology. First, *Smpec* expression is restricted to chondrocytes making it of a particular interest in cartilage and bone research. Second, the nature of SMPEC as a transmembrane protein suggests a potential involvement in chondrocyte-specific signaling pathways, and/or cell-cell or cell-matrix interactions. Thus, the SMPEC protein localization at the cell membrane at the resting and proliferating zones would enable accessibility for interaction with potential drugs at specific zones, making it of interest as a therapeutic target should it be important for normal development or disease. Third, the cross-species conservative nature of *Smpec* suggests an important evolutionary conserved function in vertebrate physiology. Finally, the fact that *Smpec* is unique and does not belong to any family member suggests that it codes for important protein with no redundancy in its function.

The objective of this research project was to further characterize the SMPEC protein, and to examine in vivo the effects of *Smpec* loss on skeletogenesis during embryonic and postnatal growth stages. We hypothesized that identifying the in vivo expression of SMPEC protein and the associated phonotype with its ablation would help in discovering its function in the cartilage and bone development in vivo**.** To address these objectives, first IHC and IF were conducted in WT mouse embryos and postnatally. We found that the SMPEC protein is expressed in all endochondral sites of bone formation involving chondrocranium, ribs, vertebra, nasal septum and Meckel cartilage of the jaw bones at the embryonic stage E18.5 which is consistent with gene expression previously identified by northern blot. Then, IF was performed on distal femur of P4 WT mice to co-localize the SMPEC. The conclusion was, SMPEC not only labeled the cell membrane of the resting and proliferating

chondrocytes but also labeled the ECM of the hypertrophic chondrocytes in which the *Smpec* gene is not expressed. The membrane localization confirmed the suggested topology for SMPEC as a transmembrane protein. The specificity of staining in all zones was verified by the total absence of signal in P4 femurs of the KO. This suggested that SMPEC is present in the cell membrane of chondrocytes until hypertrophy, at which stage SMPEC is shed off from the cell membrane and accumulates in the inter columnar septum. The presence of SMPEC in the ECM also persisted in the forming trabecular bone of the primary spongiosa, and was sometimes observed in the cortical bone of the midshaft. The mechanism by which the extracellular domain of SMPEC is released from the cell membrane is still elusive. There could be a protease expressed at the pre-hypertrophic stage that would cleave SMPEC. However, upon scanning the SMPEC primary sequence, no identifiable conserved cleavage site could be detected. This possibility of shedding could be addressed through the analysis for the presence of SMPEC in the conditioned media from costal cartilage cultures as described before (156 and 157) or through micro mass culture as described (158 and 159). Also, whether the release of the SMPEC extracellular domain into the ECM bears any functional role(s) is unknown. This is particularly interesting in light of other (unpublished) data generated in our laboratory by other member that suggested SMPEC is negatively modulating mineralization in vitro in ATDC5 chondrocytes. Its accumulation in the intercolumnar septum could be affecting mineralization of the cartilage ECM known to be happening there, but collectively the following data obtained from the KO mouse does not allow us to definitely conclude this. Further analyses such as μCT or the use of stains specific for the mineralized tissue (Von Kossa, alizarin red) will be required to assess this possibility. As a whole our IHC and IF results corroborate and further extend the data published (147). Unfortunately, these authors did not present any functional data

about SMPEC (SNORC), except for its increased gene regulation by Bone morphogenetic protein 2 (BMP2) in chondrocyte micromass cultures.

Second, a KO mouse model was generated by other member of our lab in which *Smpec* gene is completely replaced by *Lac-Z* gene. The aim of this mouse model was to determine the in vivo role of *Smpec* in skeletogenesis and in other physiological processes that could be dependent on SMPEC, if any. The efficiency of the KO was tested by whole mount X-gal staining. We expected that the expression of *Lac-Z* gene in the KO would mimics the expression of *Smpec* in the WT. In KO mice, a specific signal was detected at the ribs, limbs and mandible versus pale non specific signal in the WT, suggesting the *Lac-Z* cassette is a valid reporter of *Smpec* gene expression. This also suggested that the regulatory regions involved in the *Smpec* gene transcription were preserved in the context of the KO, and were not affected by the deletion of the entire exonic region.

Although the *Smpec* gene is not part of a family, the homozygote KO appeared normal by visual examination, reproduced normally, did not present any patterning abnormalities, and grew normally. This was disappointing as we expected a more severe phenotype. Staining the skeleton with alcian blue/alizarin red at P4 also did not reveal gross bone and cartilage differences as compared to WT littermates. Quantitative measurements of the P4 neonatal humerus revealed, however, a mild dwarfism in the KO compared to the littermate WT. As it is well known that the continual process in the epiphyseal growth plate resulted in a longitudinal growth of a long bone until the bone is fully developed, thus we focus on studying this region.

Safranin O/Fast Green staining on femur tissue sections of P4 neonatal mice of WT and KO revealed overall similarity in the PG deposit into the ECM but the *Smpec* KO exhibited hypocellularity as compared to WT in both resting and proliferating zones. This was confirmed by calculating the total number of cells in a defined area of the resting zone. Then, IHC with BrdU labeling, which labels specifically proliferating cells, was carried out to calculate the total number of cells in a defined area of the proliferating zone and the proliferation status. These measurements indicated that the total number of cells in the proliferating zone of the KO was significantly reduced compared to WT. Whether this phenotype is permanent or transient is still unknown and could be checked by repeating this procedure at later ages. If the function of SMPEC protein could be compensated by other protein(s), the dwarfism would be cured at later age whereas if the function of the SMPEC protein is unique, the phenotype will remain even at later age. Dwarfism accompanied with hypocellularity was reported before (160 and 161). We hypothesized that the hypocellularity might be due to excessive cell death in the KO compared to WT. This could be assessed by Terminal deoxynucleotidyl transferase dUTP nick end labeling (TUNEL) assay as explained before (162 and 163). Also, this hypocellularity might be due to reduction in the stem cells which committed to chondrocytic lineage. The mechanism of action is still obscure thus identifying protein(s) which interact with the SMPEC are ongoing experiments that would possibly identify pathway(s) that SMPEC is involved in. A membrane yeast two-hybrid procedure (164 and 165) performed by other member of

our group has already identified one potential membrane protein that is interacting with SMPEC.

Finally, at the molecular level, we studied the effect of *Smpec* ablation on the expression profile of marker genes known to be key for chondrogenesis and skeletogenesis. Hence, results from real-time qPCR monitoring on femur condyles and articular cartilage, showed only subtle and transient differences only in some of the target genes tested, and no clear trends could be reproducibly observed at the three ages examined (P4, 28 days, 12 months). Although performed with more limited sets of genes, primary chondrocyte cultures derived from the WT and KO ribs didn't reveal significant changes in gene expression. This suggested that *Smpec* deficiency did not significantly affect the expression pattern of those genes, and that it did not impact on cell signalling leading to gene expression. It is still possible, however, that genes other than those selected could have been altered. Maybe broader genome wide microarray hybridization experiments would be required to reveal a more discrete gene pathway signature regulated by SMPEC. Lastly, PG ACAN deposition by such cultures was indistinguishable between the WT and KO, which assessed quantitatively by alcian blue staining. This result could be interpreted that there is no major negative metabolic impact of the absence of SMPEC on chondrocytes.

On a technical perspective, it was noticed that those primary chondrocyte cultures tended to have global decrease in the gene expression of chondrogenic markers (*Acan, Col2a1* and *Col10a1*). This has been observed previously (166-168),

and is suggestive of de-differentiation. Refinement in culture conditions could be implemented to better recapitulate the chondrogenic program, such as by the addition of certain growth factors like the transforming growth factor β or other substances known to reduce the tendency of the chondrocyte to de-differentiate like insulin-transferrin-selenium (169). These modifications have been recently introduced in newer cultures but the results of those experiments will only be available in the future.

The mild phenotype observed in our *Smpec* KO mouse is interesting in light of other studies in the *Col10a1*, *Matrilin-3, Wisp3*, and *Comp* KO mice where no observable phenotypes were observed (47 and 170-172). Yet, mutations in these genes are known to cause human Chondrodysplasia syndromes (43-45 and 173-175). Thus the production of mutant proteins seemed detrimental for the cell and tissue function than the total absence of that protein (45-47). Perhaps the expression of a mutant SMPEC protein, or expressing SMPEC in another compartment (in hypertrophic chondrocytes for instancess) would exacerbate the phenotype or answer how SMPEC ectopic misexpression impacts the final stages of growth plate chondrocyte maturation, mineralization, and longitudinal growth. Alternatively, it is possible that the physiological function of SMPEC in the KO could be revealed upon a challenge or stress that could be induced upon fracture repair for example. Like other PG present in the growth plate, another unexplored possibility is that SMPEC, through its CS GAG side chain, could binds and serves as a receptor for a known or still unidentified growth factor.

Original Contribution to Science

- Characterization of *Smpec* KO mouse model.
- Test the expression profile of certain genes important of chondrogenesis and skeletogenesis in vivo and in vitro.
- *Smpec* ablation resulted in a mild dwarfism.
- *Smpec* absence resulted in hypocellularity of the resting as well as the proliferating chondrocytes of the growth plate zones.

V. References:

1. Marieb, E. N. and K. Hoehn (2007). Human Anatomy & Physiology, Pearson Benjamin Cummings.

2.Crockett, J., M. Rogers, et al. (2011). "Bone remodelling at a glance." Journal of Cell Science **124**(7): 991-998.

3. Karsenty, G. (1998). "Genetics of skeletogenesis." Developmental Genetics **22**(4): 301-313.

4. Olsen, B., A. Reginato, et al. (2000). "BONE DEVELOPMENT." Annual Review of Cell and Developmental Biology **16**(1): 191-220.

5. Taipaleenmäki, H. (2010). "Factors Regulating Chondrogenic Differentiation." Optometry and vision science **87**: 337-343.

6. Horton, W.A. (1993). "Cartilage morphology." In Extracellular Matrix and Heritable Disorder of Connective Tissue. P.M. Royce and B. Steinman, editors. Alan R. Liss, New York:73–84.

7. Goldring, M., K. Tsuchimochi, et al. (2006). "The control of chondrogenesis." Journal of Cellular Biochemistry **97**(1): 33-44.

8. Zuscik, M., M. Hilton, et al. (2008). "Regulation of chondrogenesis and chondrocyte differentiation by stress." The Journal of Clinical Investigation **118**(2): 429-438.

9. Yang, Y. (2009). "Skeletal Morphogenesis during Embryonic Development." Critical Review in Eukaryotic Gene Expression **19**(3): 197-218.

10. Karsenty, G., H. Kronenberg, et al. (2009). "Genetic Control of Bone Formation." Annual Review of Cell and Developmental Biology **25**(1): 629-648.

11. De Crombrugghe, B., V. Lefebvre, et al. (2001). "Regulatory mechanisms in the pathways of cartilage and bone formation." Current Opinion in Cell Biology **13**(6): 721-728.

12. Kronenberg, H. M. (2003). "Developmental regulation of the growth plate." Nature **423**(6937): 332-336.

13. Ballock, R. and R. O'Keefe (2003). "The Biology of the Growth Plate." The Journal of Bone & Joint Surgery **85**(4): 715-726.

14. Hunziker, E. B. (1994). "Mechanism of longitudinal bone growth and its regulation by growth plate chondrocytes." Microscopy Research and Technique **28** (6):505-519.

15. Archer, C. and P. Francis-West (2003). "The chondrocyte." The International Journal of Biochemistry & Cell Biology **35**(4): 401-404.

16. Cowell, H., E. Hunziker, and L. Rosenberg (1987). "The role of hypertrophic chondrocytes in endochondral ossification and in the development of secondary centers of ossification." Journal of Bone and Joint Surgery **69**(2):159-161.

17. Ferrara, N., H. Gerber, et al. (2003). "The biology of VEGF and its receptors." Nature Medicine **9**(6): 669-676.

18. Bi, W., J. Deng, et al. (1999). "Sox9 is required for cartilage formation." Nature Genetics **22**(1): 85-89.

19. Van de Wetering, M. and H. Clevers (1992). " Sequence-specific interaction of the HMG box proteins TCF-1 and SRY occurs within the minor groove of a Watson-Crick double helix." EMBO Journal **11**(8):3039-44.

20. Dubin, R. and H. Ostrer (1994). "Sry is a transcriptional activator." Molecular Endocrinology **8**(9): 1182-1192.

21. Giese, K., C. Kingsley, et al. (1995). "Assembly and function of a TCR alpha enhancer complex is dependent on LEF-1-induced DNA bending and multiple protein-protein interactions." Genes & Development **9**(8): 995-1008.

22. Wuelling, M. and A. Vortkamp (2010). "Transcriptional networks controlling chondrocyte proliferation and differentiation during endochondral ossification." Pediatric Nephrology **25**(4): 625-631.

23. Bell, D., K. Leung, et al. (1997). "SOX9 directly regulates the type-ll collagen gene." Nature Genetics **16**(2): 174-178.

24. Foster, J., M. Dominguez-Steglich, et al. (1994). "Campomelic dysplasia and autosomal sex reversal caused by mutations in an SRY-related gene." Nature **372**(6506): 525-530.

25. Wagner, T., J. Wirth, et al. (1994). "Autosomal sex reversal and campomelic dysplasia are caused by mutations in and around the SRY-related gene SOX9." Cell **79**(6): 1111-1120.

26. Bi, W., W. Huang, et al. (2001). "Haploinsufficiency of Sox9 results in defective cartilage primordia and premature skeletal mineralization." Proceedings of the National Academy of Sciences **98**(12): 6698-6703.

27. Strom, C. and W. Upholt (1984). "Isolation and characterization of genomic clones corresponding to the human type II procollagengene." Nucleic Acids Research **12**(2): 1025-1038.

28. Cheah, K., N. Stoker, et al. (1985). "Identification and characterization of the human type II collagen gene (COL2A1)." Proceedings of the National Academy of Sciences **82**(9): 2555-2559.

29. Gelse, K., E. Pöschl, et al. (2003). "Collagens—structure, function, and biosynthesis." Advanced Drug Delivery Reviews **55**(12): 1531-1546.

30. Mayne, R. (1989). "Cartilage collagens. What Is Their Function, and Are They Involved in Articular Disease?" Arthritis & Rheumatism **32**(3): 241-246.

31. Eyre, D. (2002). "Collagen of articular cartilage." Arthritis research **4**(1): 30-35

32. Godfrey, M. and D. Hollister (1988). "Type II achondrogenesis-hypochondrogenesis: identification of abnormal type II collagen." American Journal of Human Genetics **43**(6): 904-913.

33. Knowlton, R. G., P. Katzenstein, et al. (1989). "Genetic linkage of the type II procollagen gene to primary generalized osteoarthritis with chondrodysplasia." Cytogenetics and Cell Genetics 51: 1024 only.

34. Knowlton, R., P. Katzenstein, et al. (1990). "Genetic Linkage of a Polymorphism in the Type II Procollagen Gene (COL2A1) to Primary Osteoarthritis Associated with Mild Chondrodysplasia." New England Journal of Medicine **322**(8): 526-530.

35. Ala-Kokko, L., C. Baldwin, et al. (1990). "Single base mutation in the type II procollagen gene (COL2A1) as a cause of primary osteoarthritis associated with a mild chondrodysplasia." Proceedings of the National Academy of Sciences **87**(17): 6565-6568.

36. Wilkin, D., A. Artz, et al. (1999). "Small deletions in the type II collagen triple helix produce Kniest dysplasia." American Journal of Medical Genetics **85**(2): 105-112.

37. Wilkin, D., R. Liberfarb, et al. (2000). "Rapid determination of COL2A1 mutations in individuals with Stickler syndrome: Analysis of potential premature termination codons." American Journal of Medical Genetics **94**(2): 141-148.

38. Körkkö, J., D. Cohn, et al. (2000). "Widely distributed mutations in the COL2A1 gene produce achondrogenesis type II/hypochondrogenesis." American Journal of Medical Genetics **92**(2): 95-100.

39. Mundlos, S. and B. Olsen (1997). "Heritable diseases of the skeleton. Part II: Molecular insights into skeletal development-matrix components and their homeostasis." The FASEB Journal **11**(4): 227-233.

40. Zheng, Q., G. Zhou, et al. (2003). "Type X Collagen gene regulation by Runx2 contributes directly to its hypertrophic chondrocyte specific expression in vivo." Journal of Cell Biology **162**(5): 833-842.

41. Inada, M., T. Yasui, et al. (1999). "Maturational disturbance of chondrocytes in Cbfa1-deficient mice." Developmental Dynamics **214**(4): 279-290.

42. Kim, I., F. Otto, et al. (1999). "Regulation of chondrocyte differentiation by Cbfa1." Mechanisms of Development **80**(2): 159-170.

43. Warman, M., M. Abbott, et al. (1993). "A type X collagen mutation causes Schmid metaphyseal chondrodysplasia." Nature Genetics **5**(1): 79-82.

44. Bateman, J., R. Wilson, et al. (2005). "Mutations of COL10A1 in Schmid metaphyseal chondrodysplasia." Human Mutation **25**(6): 525-534.

45. Ho, M., K. Tsang, et al. (2007). "COL10A1 nonsense and frame-shift mutations have a gain-of-function effect on the growth plate in human and mouse metaphyseal chondrodysplasia type Schmid." Human Molecular Genetics **16**(10): 1201-1215.

46. Jacenko, O., P. LuValle, et al. (1993). "Spondylometaphyseal dysplasia in mice carrying a dominant negative mutation in a matrix protein specific for cartilage-to-bone transition." Nature **365**(6441): 56-61.

47. Rosati, R., G. Horan, et al. (1994). "Normal long bone growth and development in type X collagen-null mice." Nature Genetics **8**(2): 129-135.

48. Mäkitie, O., M. Susic, et al. (2010). "Early-onset metaphysea chondrodysplasia type Schmid associated with a COL10A1 frame-shift mutation and impaired trimerization of wild-type α1(X) protein chains."Journal of Orthopaedic Research **28**(11): 1497-1501.

49. Harris, H. (1990). "The human alkaline phosphatases: What we know and what we don't know." Clinica Chimica Acta **186**(2): 133-150.

50. Weiss, M. , P. Henthorn, et al. (1986). "Isolation and characterization of a cDNA encoding a human liver/bone/kidney-type alkaline phosphatase." Proceedings of the National Academy of Sciences **83**(19): 7182-7186.

51. Rodan, G., J. Heath, et al. (1988). "Diversity of the osteoblastic phenotype." Ciba Foundation symposium 136:78-91.

52. Stein, G. and J. Lian (1993). "Molecular Mechanisms Mediating Proliferation

/Differentiation Interrelationships During Progressive Development of the Osteoblast Phenotype." Endocrine Reviews **14**(4): 424-442.

53. Descalzi F., C. Gentili, et al. (1992). "Hypertrophic chondrocytes undergo further differentiation in culture." The Journal of Cell Biology **117**(2): 427-435.

54. Anderson HC. (1995). "Molecular biology of matrix vesicles." Clinical Orthopaedics and Related Research (314):266-280.

55.Weiss, M., D. Cole, et al. (1988). "A missense mutation in the human liver /bone /kidney alkaline phosphatase gene causing a lethal form of hypophosphatasia." Proceedings of the National Academy of Sciences **85**(20): 7666-7669.

56. Henthorn, P., M. Raducha, et al. (1992). "Different missense mutations at the tissue-nonspecific alkaline phosphatase gene locus in autosomal recessively inherited forms of mild and severe hypophosphatasia." Proceedings of the National Academy of Sciences **89**(20): 9924-9928.

57. Henthorn, P. and M. Whyte (1992). "Missense mutations of the tissue-nonspecific alkaline phosphatase gene in hypophosphatasia." Clinical Chemistry **38**(12): 2501-2505.

58. Zurutuza, L., F. Muller, et al. (1999). "Correlations of Genotype and Phenotype in Hypophosphatasia." Human Molecular Genetics **8**(6): 1039-1046.

59. Mornet, E. (2000). "Hypophosphatasia: The mutations in the tissue-nonspecific alkaline phosphatase gene." Human Mutation **15**(4): 309-315.

60. Lia-Baldini, A., F. Muller, et al. (2001). "A molecular approach to dominance in hypophosphatasia." Human Genetics **109**(1): 99-108.

61. Herasse, M., M. Spentchian, et al. (2003). "Molecular study of three cases of odontohypophosphatasia resulting from heterozygosity for mutations in the tissue non-specific alkaline phosphatase gene." Journal of Medical Genetics **40**(8): 605-609.

62. Wennberg, C., L. Hessle, et al. (2000). "Functional Characterization of Osteoblasts and Osteoclasts from Alkaline Phosphatase Knockout Mice." Journal of Bone and Mineral Research **15**(10): 1879-1888.

63. Hessle, L., K. Johnson, et al. (2002). "Tissue-nonspecific alkaline phosphatase and plasma cell membrane glycoprotein-1 are central antagonistic regulators of bone mineralization." Proceedings of the National Academy of Sciences **99**(14): 9445-9449.

64. Zhang, Y., M. Brown, et al. (2007). "Investigation of the role of ENPP1 and TNAP genes in chondrocalcinosis." Rheumatology **46**(4): 586-589.

65. Ho, A., M. Johnson, et al. (2000). "Role of the Mouse ank Gene in Control of Tissue Calcification and Arthritis." Science **289**(5477): 265-270.

66. Zaka, R. and C. Williams (2006). "Role of the progressive ankylosis gene in cartilage mineralization." Current Opinion in Rheumatology **18**(2): 181-186.

67. Nürnberg, P., S. Tinschert, et al. (1997). "The Gene for Autosomal Dominant Craniometaphyseal Dysplasia Maps to Chromosome 5p and Is Distinct from the Growth Hormone-Receptor Gene." American Journal of Human Genetics **61**(4): 918-923.

68. Nurnberg, P., H. Thiele, et al. (2001). "Heterozygous mutations in ANKH, the

human ortholog of the mouse progressive ankylosis gene, result in craniometaphyseal dysplasia." Nature Genetics **28**(1): 37-41.

69. Reichenberger, E., V. Tiziani, et al. (2001). "Autosomal Dominant Craniometaphyseal Dysplasia Is Caused by Mutations in the Transmembrane Protein ANK." American Journal of Human Genetics **68**(6): 1321-1326.

70. Pendleton, A., M. Johnson, et al. (2002). "Mutations in ANKH Cause Chondrocalcinosis." American Journal of Human Genetics **71**(4): 933-940.

71. Williams, C., Y. Zhang, et al. (2002). "Autosomal Dominant Familial Calcium Pyrophosphate Dihydrate Deposition Disease Is Caused by Mutation in the Transmembrane Protein ANKH." American Journal of Human Genetics **71**(4): 985-991.

72. Williams, C., A. Pendleton, et al. (2003). "Mutations in the amino terminus of ANKH in two US families with calcium pyrophosphate dihydrate crystal deposition disease." Arthritis & Rheumatism **48**(9): 2627-2631.

73. Gurley K., R. Reimer, et al. (2006). "Biochemical and Genetic Analysis of ANK in Arthritis and Bone Disease." American Journal of Human Genetics **79**(6): 1017-1029.

74. Baynam, G., J. Goldblatt, et al. (2009). "Craniometaphyseal dysplasia and chondrocalcinosis cosegregating in a family with an ANKH mutation." American Journal of Medical Genetics Part A **149A**(6): 1331-1333.

75. Bello, V., J. Goding, et al. (2001). "Characterization of a Di-leucine–based Signal in the Cytoplasmic Tail of the Nucleotide-pyrophosphatase NPP1 That Mediates

Basolateral Targeting but not Endocytosis." Molecular Biology of the Cell **12**(10): 3004-3015.

76. Yano, Y., Y. Hayashi, et al. (2004). "Expression and localization of ecto-nucleotide pyrophosphatase/phosphodiesterase I-1 (E-NPP1/PC-1) and -3 (E-NPP3/CD203c/PD-Iβ/B10/gp130RB13-6) in inflammatory and neoplastic bile duct diseases." Cancer Letters **207**(2): 139-147.

77. Maddux, B. and I. Goldfine (2000). "Membrane glycoprotein PC-1 inhibition of insulin receptor function occurs via direct interaction with the receptor alpha-subunit." Diabetes **49**(1): 13-19.

78. Harahap, A. and J. Goding (1988). "Distribution of the murine plasma cell antigen PC-1 in non-lymphoid tissues." The Journal of Immunology **141**(7): 2317-2320.

79. Rutsch, F., N. Ruf, et al. (2003). "Mutations in ENPP1 are associated with 'idiopathic' infantile arterial calcification." Nature Genetics **34**(4): 379-381.

80. Cheng, K., M. Chen, et al. (2005). "Generalized arterial calcification of infancy: Different clinical courses in two affected siblings." American Journal of Medical Genetics Part A **136A**(2): 210-213.

81. Ruf, N., B. Uhlenberg, et al. (2005). "The mutational spectrum of ENPP1 as arising after the analysis of 23 unrelated patients with generalized arterial calcification of infancy (GACI)." Human Mutation **25**(1): 98 only.

82. Rutsch, F., P. Böyer, et al. (2008). "Hypophosphatemia, Hyperphosphaturia, and Bisphosphonate Treatment Are Associated With Survival Beyond Infancy in

Generalized Arterial Calcification of Infancy." Circulation: Cardiovascular Genetics **1**(2): 133-140.

83. Dlamini, N., M. Splitt, et al. (2009). "Generalized arterial calcification of infancy: Phenotypic spectrum among three siblings including one case without obvious arterial calcifications." American Journal of Medical Genetics Part A **149A**(3): 456-460.

84. Nitschke, Y., G. Baujat, et al. (2012). "Generalized Arterial Calcification of Infancy and Pseudoxanthoma Elasticum Can Be Caused by Mutations in Either ENPP1 or ABCC6." American Journal of Human Genetics **90**(1): 25-39.

85. Nakamura, I., S. Ikegawa, et al. (1999). "Association of the human NPPS gene with ossification of the posterior longitudinal ligament of the spine (OPLL)." Human Genetics **104**(6): 492-497.

86. Koshizuka, Y., H. Kawaguchi, et al. (2002). "Nucleotide Pyrophosphatase Gene Polymorphism Associated With Ossification of the Posterior Longitudinal Ligament of the Spine." Journal of Bone and Mineral Research **17**(1): 138-144.

87. Horikoshi, T., K. Maeda, et al. (2006). "A large-scale genetic association study of ossification of the posterior longitudinal ligament of the spine." Human Genetics **119**(6): 611-616.

88. Cancela, L., C. Hsieh, et al. (1990). "Molecular structure, chromosome assignment, and promoter organization of the human matrix Gla protein gene." Journal of Biological Chemistry **265**(25): 15040-15048.

89. Laizé, V., P. Martel, et al. (2005). "Evolution of Matrix and Bone γ-Carboxyglutamic Acid Proteins in Vertebrates." Journal of Biological Chemistry **280**(29): 26659-26668.

90. Luo, G., P. Ducy, et al. (1997). "Spontaneous calcification of arteries and cartilage in mice lacking matrix GLA protein." Nature **386**(6620): 78-81.

91. Newman, B., L. Gigout, et al. (2001). "Coordinated expression of matrix Gla protein is required during endochondral ossification for chondrocyte survival." The Journal of Cell Biology **154**(3): 659-666.

92. Li, Q., Q. Jiang, et al. (2007). "Pseudoxanthoma elasticum: Reduced γ-glutamyl carboxylation of matrix gla protein in a mouse model (Abcc6−/−)." Biochemical and Biophysical Research Communications **364**(2): 208-213.

93. Price, P., S. Faus, et al. (1998). "Warfarin Causes Rapid Calcification of the Elastic Lamellae in Rat Arteries and Heart Valves." Arteriosclerosis, Thrombosis, and Vascular Biology **18**(9): 1400-1407.

94. Yagami, K., J. Suh, et al. (1999). "Matrix Gla Protein Is a Developmental Regulator of Chondrocyte Mineralization And, When Constitutively Expressed, Blocks Endochondral and Intramembranous Ossification in the Limb." The Journal of Cell Biology **147**(5): 1097-1108.

95. Munroe, P., R. Olgunturk, et al. (1999). "Mutations in the gene encoding the human matrix Gla protein cause Keutel syndrome." Nature Genetics **21**(1): 142-144.

96. Hirano, H., Y. Ezura, et al. (2003). "Association of natural tooth loss with genetic variation at the human matrix Gla protein locus in elderly women." Journal of Human Genetics **48**(6): 288-292.

97. Ogbureke, K. and L. Fisher (2007). "SIBLING Expression Patterns in Duct Epithelia Reflect the Degree of Metabolic Activity." Journal of Histochemistry & Cytochemistry **55**(4): 403-409.

98. Saavedra, R, S. Kimbro, et al. (1995). "Gene Expression and Phosphorylation of Mouse Osteopontina." Annals of the New York Academy of Sciences **760**(1): 35-43.

99. Lasa, M., P. Chang, et al. (1997). "Phosphorylation of Osteopontin by Golgi Apparatus Casein Kinase." Biochemical and Biophysical Research Communications **240**(3): 602-605.

100. Oldberg, A., A. Franzén, et al. (1986). "Cloning and sequence analysis of rat bone sialoprotein (osteopontin) cDNA reveals an Arg-Gly-Asp cell-binding sequence." Proceedings of the National Academy of Sciences **83**(23): 8819-8823.

101. Shanmugam, V., I. Chackalaparampil, et al. (1997). "Altered Sialylation of Osteopontin Prevents Its Receptor-Mediated Binding on the Surface of Oncogenically Transformed tsB77 Cells." Biochemistry **36**(19): 5729-5738.

102. Nagata, T., R. Todescan, et al. (1989). "Sulphation of secreted phosphoprotein I (SPPI, osteopontin) is associated with mineralized tissue formation." Biochemical and Biophysical Research Communications **165**(1): 234-240.

103. Prince, C., D. Dickie, et al. (1991). "Osteopontin, a substrate for transglutaminase and Factor XIII activity." Biochemical and Biophysical Research Communications **177**(3): 1205-1210.

104. Reinholt, F., K. Hultenby, et al. (1990). "Osteopontin--a possible anchor of osteoclasts to bone." Proceedings of the National Academy of Sciences **87**(12): 4473-4475.

105. Bautista, D., J. Xuan, et al. (1994). "Inhibition of Arg-Gly-Asp (RGD)-mediated cell adhesion to osteopontin by a monoclonal antibody against osteopontin." Journal of Biological Chemistry **269**(37): 23280-23285.

106. Katayama, Y., C. House, et al. (1998). "Casein kinase 2 phosphorylation of recombinant rat osteopontin enhances adhesion of osteoclasts but not osteoblasts." Journal of Cellular Physiology **176**(1): 179-187.

107. Brown, L., B. Berse, et al. (1992). "Expression and distribution of osteopontin in human tissues: widespread association with luminal epithelial surfaces." Molecular Biology of the Cell **3**(10): 1169-1180.

108. Young, M., J. Kerr, et al. (1990). "cDNA cloning, mRNA distribution and heterogeneity, chromosomal location, and RFLP analysis of human osteopontin (OPN)." Genomics **7**(4): 491-502.

109. Gerstenfeld, L. and F. Shapiro (1996). "Expression of bone-specific genes by hypertrophic chondrocytes: Implications of the complex functions of the hypertrophic chondrocyte during endochondral bone development." Journal of Cellular Biochemistry **62**(1): 1-9.

110. Merry, K., R. Dodds, et al. (1993). "Expression of osteopontin mRNA by osteoclasts and osteoblasts in modelling adult human bone." Journal of Cell Science **104**(4): 1013-1020.

111. Tezuka, K., T. Sato, et al. (1992). "Identification of osteopontin in isolated rabbit osteoclasts." Biochemical and Biophysical Research Communications **186**(2): 911-917.

112. Asou, Y., S. Rittling, et al. (2001). "Osteopontin Facilitates Angiogenesis, Accumulation of Osteoclasts, and Resorption in Ectopic Bone." Endocrinology **142**(3): 1325-1332.

113. Pampena, D., K. Robertson, et al. (2004). "Inhibition of hydroxyapatite formation by osteopontin phosphopeptides." The Biochemical Journal **378**(3): 1083-1087.

114. Bülow, H. and O. Hobert (2006). "The Molecular Diversity of Glycosaminoglycans Shapes Animal Development." Annual Review of Cell and Developmental Biology **22**(1): 375-407.

115. Arambawatta, A., T. Yamamoto, et al. (2005). "Immunohistochemical characterization of noncollagenous matrix molecules on the alveolar bone surface at the initial principal fiber attachment in rat molars." Annals of Anatomy - Anatomischer Anzeiger **187**(1): 77-87.

116. Sisu, E., C. Flangea, et al. (2011). "Modern developments in mass spectrometry of chondroitin and dermatan sulfate glycosaminoglycans." Amino Acids **41**(2): 235-256.

117. Couchman, J. and C. Pataki (2012). "An Introduction to Proteoglycans and Their Localization." Journal of Histochemistry & Cytochemistry **60**(12): 885-897.

118. Knudson, C. and W. Knudson (2001). "Cartilage proteoglycans." Seminars in Cell & Developmental Biology **12**(2): 69-78.

119. Happonen, K. E., C. Fürst, et al. (2012). "PRELP Protein Inhibits the Formation of the Complement Membrane Attack Complex." Journal of Biological Chemistry **287**(11): 8092-8100.

120. Kalamajski, S. and Å. Oldberg (2010). "The role of small leucine-rich proteoglycans in collagen fibrillogenesis." Matrix Biology **29**(4): 248-253.

121. Chuang, C., M. Lord, et al. (2010). "Heparan Sulfate-Dependent Signaling of Fibroblast Growth Factor 18 by Chondrocyte-Derived Perlecan." Biochemistry **49**(26): 5524-5532.

122. Cortes, M., A. Baria, et al. (2009). "Sulfation of chondroitin sulfate proteoglycans is necessary for proper Indian hedgehog signaling in the developing growth plate." Development **136**(10): 1697-1706.

123. Fisher, M., Y. Li, et al. (2006). "Heparan sulfate proteoglycans including syndecan-3 modulate BMP activity during limb cartilage differentiation." Matrix Biology **25**(1): 27-39.

124. Li, S., C. Shimono, et al. (2010). "Activin A Binds to Perlecan through Its Pro-region That Has Heparin/Heparan Sulfate Binding Activity." Journal of Biological Chemistry **285**(47): 36645-36655.

125. Smith, S., L. West, et al. (2007). "Heparan and chondroitin sulfate on growth plate perlecan mediate binding and delivery of FGF-2 to FGF receptors." Matrix Biology **26**(3): 175-184.

126. Domowicz, M., M. Cortes, et al. (2009). "Aggrecan modulation of growth plate morphogenesis." Developmental Biology **329**(2): 242-257.

127. Glumoff, V., M. Savontaus, et al. (1994). "Analysis of aggrecan and tenascin gene expression in mouse skeletal tissues by Northern and in situ hybridization using species specific cDNA probes." Biochimica et Biophysica Acta (BBA) - Gene Structure and Expression **1219**(3): 613-622.

128. Gleghorn, L., R. Ramesar, et al. (2005). "A Mutation in the Variable Repeat Region of the Aggrecan Gene (AGC1) Causes a Form of Spondyloepiphyseal Dysplasia Associated with Severe, Premature Osteoarthritis." American Journal of Human Genetics **77**(3): 484-490.

129. Tompson, S., B. Merriman, et al. (2009). "A Recessive Skeletal Dysplasia, SEMD Aggrecan Type, Results from a Missense Mutation Affecting the C-Type Lectin Domain of Aggrecan." American Journal of Human Genetics **84**(1): 72-79.

130. Stattin, E., F. Wiklund, et al. (2010). "A Missense Mutation in the Aggrecan C-type Lectin Domain Disrupts Extracellular Matrix Interactions and Causes Dominant Familial Osteochondritis Dissecans." American Journal of Human Genetics **86**(2): 126-137.

131. Watanabe, H., K. Kimata, et al. (1994). "Mouse cartilage matrix deficiency (cmd) caused by a 7 bp deletion in the aggrecan gene." Nature Genetics **7**(2): 154-157.

132. Watanabe, H., K. Nakata, et al. (1997). "Dwarfism and age-associated spinal degeneration of heterozygote cmd mice defective in aggrecan." Proceedings of the National Academy of Sciences **94**(13): 6943-6947.

133. Watanabe, H. and Y. Yamada (2002). "Chondrodysplasia of gene knockout mice for aggrecan and link protein." Glycoconjugate Journal **19**(4-5): 269-273.

134. Day, J., A. Olin, et al. (2004). "Alternative Splicing in the Aggrecan G3 Domain Influences Binding Interactions with Tenascin-C and Other Extracellular Matrix Proteins." Journal of Biological Chemistry **279**(13): 12511-12518.

135. Maeda, Y., E. Nakamura, et al. (2007). "Indian Hedgehog produced by postnatal chondrocytes is essential for maintaining a growth plate and trabecular bone." Proceedings of the National Academy of Sciences **104**(15): 6382-6387.

136. Yan, D. and X. Lin (2009). "Shaping morphogen gradients by proteoglycans." Cold Spring Harbor perspectives in biology **1**(3): a002493.

137. Jay, G., D. Britt, et al. (2000). "Lubricin is a product of megakaryocyte stimulating factor gene expression by human synovial fibroblasts." The Journal of Rheumatology **27**(3): 594-600.

138. Liu, T., W. Qian, et al. (2005). "Human Plasma N-Glycoproteome Analysis by Immunoaffinity Subtraction, Hydrazide Chemistry, and Mass Spectrometry." Journal of Proteome Research **4**(6): 2070-2080.

139. Ikegawa, S., M. Sano, et al. (2000). "Isolation, characterization and mapping of the mouse and human PRG4 (proteoglycan 4) genes." Cytogenetics and Cell Genetics **90**(3-4): 291-297.

140. Rhee, D., J. Marcelino, et al. (2005). "The secreted glycoprotein lubricin protects cartilage surfaces and inhibits synovial cell overgrowth." The Journal of Clinical Investigation **115**(3): 622-631.

141. Marcelino, J., J. Carpten, et al. (1999). "CACP, encoding a secreted proteoglycan, is mutated in camptodactyly-arthropathy-coxa vara-pericarditis syndrome." Nature Genetics **23**(3): 319-322.

142. Theocharis, A., S. Skandalis, et al. (2010). "Proteoglycans in health and disease: novel roles for proteoglycans in malignancy and their pharmacological targeting." FEBS Journal **277**(19): 3904-3923.

143. Choi, Y., H. Chung, et al. (2011). "Syndecans as cell surface receptors: Unique structure equates with functional diversity." Matrix Biology **30**(2): 93-99.

144. Pap, T. and J. Bertrand (2013). "Syndecans in cartilage breakdown and synovial inflammation." Nature Reviews Rheumatology **9**(1): 43-55.

145. Manon-Jensen, T., Y. Itoh, et al. (2010). "Proteoglycans in health and disease: the multiple roles of syndecan shedding." FEBS Journal **277**(19): 3876-3889.

146. Moffatt, P., P. Salois, et al. (2002). "Engineered viruses to select genes encoding secreted and membrane‐bound proteins in mammalian cells." Nucleic Acids Research **30**(19): 4285-4294.

147. Heinonen, J., H. Taipaleenmäki, et al. (2011). "Snorc is a novel cartilage specific

small membrane proteoglycan expressed in differentiating and articular chondrocytes." Osteoarthritis and cartilage **19**(8): 1026-1035.

148. Embree, M., M. Ono, et al. (2011). "Role of Subchondral Bone during Early-stage Experimental TMJ Osteoarthritis." Journal of Dental Research **90**(11): 1331-1338.

149. Ito, T., M. Seldin, et al. (2000). "Gene structure and chromosome mapping of mouse transcription elongation factor S-II (Tcea1)." Gene **244**(1–2): 55-63.

150. Zangala, T. (2007). "Isolation of Genomic DNA from Mouse Tails." Journal of Visualized Experiments (6): e246.

151. Schrickel, J., M. Kreuzberg, et al. (2009). "Normal impulse propagation in the atrioventricular conduction system of Cx30.2/Cx40 double deficient mice." Journal of Molecular and Cellular Cardiology **46**(5): 644-652.

152. Loughna, S. and D. Henderson (2007). Methodologies for Staining and Visualisation of β-Galactosidase in Mouse Embryos and Tissues. Reporter Genes. D. Anson, Humana Press. **411:** 1-11.

153. McLeod, M. (1980). "Differential staining of cartilage and bone in whole mouse fetuses by alcian blue and alizarin red S." Teratology **22**(3): 299-301.

154. Lee, E., L. Lamplugh, et al. (2009). "Neoepitopes reveal the features of type II collagen cleavage and the identity of a collagenase involved in the transformation of the epiphyses anlagen in development." Developmental Dynamics **238**(6): 1547-1563.

155.Gosset, M., F. Berenbaum, et al. (2008). "Primary culture and phenotyping of murine chondrocytes." Nature Protocols **3**(8): 1253-1260.

156. Chevallet, M., H. Diemer, et al. (2007). "Toward a better analysis of secreted proteins: the example of the myeloid cells secretome." Proteomics **7**(11): 1757-1770.

157. Finoulst, I., P. Vink, et al. (2011). "Identification of low abundant secreted proteins and peptides from primary culture supernatants of human T-cells." Journal of Proteomics **75**(1): 23-33.

158. Kameda, T., C. Koike, et al. (2000). "Analysis of cartilage maturation using micromass cultures of primary chondrocytes." Development, Growth & Differentiation **42**(3): 229-236.

159. Morgan, T., X. Xu, et al. (2005). "Evaluation of chondrocyte micromass culture for the study of cartilage degradation." Arthritis Research & Therapy **7**(Suppl 1): 1-2.

160. Horn, D., E. Rupprecht, et al. (2001). "Anauxetic dysplasia, a spondylometaepiphyseal dysplasia with extreme dwarfism." Journal of Medical Genetics **38**(4): 262-265.

161. Wang, G., Q. Yan, et al. (2011). "Inducible nitric oxide synthase–nitric oxide signaling mediates the mitogenic activity of Rac1 during endochondral bone growth." Journal of Cell Science **124**(20): 3405-3413.

162. Labat-Moleur, F., C. Guillermet, et al. (1998). "TUNEL Apoptotic Cell Detection in Tissue Sections: Critical Evaluation and Improvement." Journal of Histochemistry & Cytochemistry **46**(3): 327-334.

163. Chen, C., N. Burton-Wurster, et al. (2001). "Chondrocyte necrosis and apoptosis in impact damaged articular cartilage." Journal of Orthopaedic Research **19**(4): 703-711.

164. Stagljar, I., C. Korostensky, et al. (1998). "A genetic system based on split-ubiquitin for the analysis of interactions between membrane proteins in vivo." Proceedings of the National Academy of Sciences **95**(9): 5187-5192.

165. Thaminy, S., J. Miller, et al. (2004). The Split-Ubiquitin Membrane-Based Yeast Two-Hybrid System. Protein-Protein Interactions. H. Fu, Humana Press. **261:** 297-312.

166. Schnabel, M., S. Marlovits, et al. (2002). "Dedifferentiation-associated changes in morphology and gene expression in primary human articular chondrocytes in cell culture." Osteoarthritis and Cartilage **10**(1): 62-70.

167. Karlsen, T., A. Shahdadfar, et al. (2011). "Human primary articular chondrocytes, chondroblasts-like cells, and dedifferentiated chondrocytes: differences in gene, microRNA, and protein expression and phenotype." Tissue Engineering Part C: Methods **17**(2): 219-27.

168. Hong, E. and A. Reddi (2012). "Dedifferentiation and Redifferentiation of Articular Chondrocytes from Surface and Middle Zones: Changes in MicroRNAs-221/-222, -140, -143/-145 Expression." Tissue Engineering Part A: Methods **19**(7-8):1015-1022.

169. Chua, K., B. Aminuddin, et al. (2005). "Insulin-transferrin-selenium prevent human chondrocyte dedifferentiation and promote the formation of high quality tissue engineered human hyaline cartilage." European Cells & Materials Journal **9**: 58-67.

170. Ko, Y., B. Kobbe, et al. (2004). "Matrilin-3 Is Dispensable for Mouse Skeletal Growth and Development." Molecular and Cellular Biology **24**(4): 1691-1699.

171. Kutz, W., Y. Gong, et al. (2005). "WISP3, the Gene Responsible for the Human Skeletal Disease Progressive Pseudorheumatoid Dysplasia, Is Not Essential for Skeletal Function in Mice." Molecular and Cellular Biology **25**(1): 414-421.

172. Svensson, L., A. Aszódi, et al. (2002). "Cartilage Oligomeric Matrix Protein-Deficient Mice Have Normal Skeletal Development." Molecular and Cellular Biology **22**(12): 4366-4371.

173. Briggs, M., S. Hoffman, et al. (1995). "Pseudoachondroplasia and multiple epiphyseal dysplasia due to mutations in the cartilage oligomeric matrix protein gene." Nature Genetics **10**(3): 330-336.

174. Chapman, K., G. Mortier, et al. (2001). "Mutations in the region encoding the von Willebrand factor A domain of matrilin-3 are associated with multiple epiphyseal dysplasia." Nature Genetics **28**(4): 393-396.

175. Hurvitz, J., W. Suwairi, et al. (1999). "Mutations in the CCN gene family member WISP3 cause progressive pseudorheumatoid dysplasia." Nature Genetics **23**(1): 94-98.

APPENDIX A

List of Oral and Poster Presentations

1. Oral Presentation at Genetics Research lab meeting, Shriners Hospital, Conference Room, Nov. 16th, 2012.

2. Oral Presentation at the European Calcified Tissue Society 39th Annual Congress; Stockholm, Sweden, May, 19–23 rd, 2012.

3. Oral Presentation at the Human Genetics Research Day. Meakins Amphitheatre, McIntyre Medical Building, McGill University; June 21st, 2012.

4. Poster Presentation at the Gordon in bones and teeth. Les Diablerets, Switzerland; June, 2011.

APPENDIX B

Published Abstract

1. Human Genetics Research Day, McGill University, June 2012

Characterization of a novel small membrane protein expressed in chondrocytes.
Latifa Aljebali and Pierre Moffatt

Cartilage is the first skeletal tissue formed during embryonic development and is a template for endochondral bone formation. Although in the last few years, much has been learned about the mechanisms that regulate the formation of the skeletal tissues, novel genes are still being identified and studied. Among those is *Smpec* (small membrane protein expressed in chondrocytes) which was identified by our group from a screen of cDNA encoding secreted and membrane proteins. The *Smpec* gene is located on mouse chromosome 1, composed of 3 exons and well conserved among 20 different species examined (mammals, birds, amphibians, reptiles). Northern blotting on embryonic and 3-week old tissues from mice revealed that *Smpec* was highly expressed and restricted to the developing limbs, and to long bones in 3-week old mice. In situ hybridization and immunohistochemistry revealed SMPEC is expressed and produced specifically in chondrocytes. SMPEC is a transmembrane protein without any identifiable functional motifs or homologies to known proteins except for the presence of a CS GAG chain attached to serine 44. At this stage the role of SMPEC in chondrogenesis and growth plate is unknown thus we created a KO mouse to study its function in vivo. Alcian blue /alizarin red staining, which stains cartilage and bone respectively, was performed on arms of 4 days WT and KO mice and there were no qualitative differences in staining intensity either in bone or cartilage

between genotype. However, quantitative measurements indicted that the humeri were all statistically reduced in length by 10.4%. This indicates that loss of *Smpec* results in mild dwarfism in mice and that its function cannot be compensate by other genes. Ongoing experiments are aimed at elucidating more precisely at the cellular and molecular levels the defect in growth plate of long bones.